

# Creation of a Full-Core HTR Benchmark with the Fort St. Vrain Initial Core and Assessment of Uncertainties in the FSV Fuel Composition and Geometry

---

## Reactor Concepts (Gen IV)

**Dr. William Martin**  
University of Michigan

**In collaboration with:**  
General Atomics  
Studsvik-Scandpower

Madeline Feltus, Federal POC  
David Nigg, Technical POC

Creation of a Full-core HTR Benchmark  
with the Fort St. Vrain Initial Core  
and  
Assessment of Uncertainties in the  
FSV Fuel Composition and Geometry

Final Report

DE-AC07-05ID14517

Project 09-771

William R. Martin, PI  
John C. Lee, co-PI

Alan Baxter, General Atomics, co-PI  
Chuck Wemple, Studsvik of America, co-PI

Ben Betzler  
Timothy Burke  
Wilson Pappo  
Andrew Pavlou  
Eva Sunny

University of Michigan  
Department of Nuclear Engineering and Radiological Sciences  
Ann Arbor, MI 48109-2104

June 2012

## Table of Contents

List of Figures .....	4
List of Tables .....	5
Abstract .....	7
I. Introduction .....	8
II. Original Project Scope.....	8
III. Modified Project Scope.....	10
IV. Uncertainties in the Geometry and Composition of the Initial FSV Core.....	12
A. Introduction .....	12
B. Description of FSV core .....	12
C. Description of uncertainties in the geometry and composition data.....	13
1. Uncertainty in relative numbers of small and large kernels .....	13
2. Uncertainty in kernel diameters .....	13
3. Uncertainty in Th/U ratio .....	14
4. Uncertainty in the buffer thickness .....	15
5. Uncertainty in the fabrication records .....	15
6. Change in contract scope .....	15
V. Development of the FSV Benchmark Suite (Task 1) .....	15
A. Summary.....	15
B. Visit to GA and preliminary FSV model.....	16
C. Python script to generate MCNP input files for FSV.....	17
D. Automated fuel loading verification with MCNP.....	17
E. Methodology for coupled NTH analysis using MCNP5 and RELAP5-3D .....	18
F. Confirmation of FSV fuel loadings by analyzing GA fabrication records .....	19
G. Construct benchmark MCNP5 models and compare with GA results (Task 1.5) .....	19
1. Cold, clean FSV core configuration .....	19
2. Initial FSV core at 70% power .....	21
H. Simulation of FSV subcriticality measurements (Task 1.6) .....	25
I. MCNP5 analyses of FSV fuel element (Tasks 1.7-1.9) .....	29
VI. Comparison of MCNP5 with HELIOS for FSV Fuel Elements (Task 2) .....	31
A. Summary .....	31
B. HELIOS analysis and comparison with MCNP5 (Tasks 2.1 and 2.2).....	31
C. Discussion of HELIOS and MCNP5 differences (Tasks 2.1 and 2.2) .....	32
VII. Sensitivity Analyses for FSV Fuel Parameters (Task 3) .....	32
A. Summary .....	32
B. Development of reference 4-diameter model .....	34

C. Equivalent 2-diameter model .....	35
D. Continuous diameter model .....	35
E. Stochastic compact model .....	38
F. Results of sensitivity studies for fuel compacts (Tasks 3., 3.2, and 3.4) .....	39
G. Results of sensitivity studies for fuel columns .....	40
H. Determine sensitivity of MCNP5 results to kernel diameter PDF (Task 3.2) .....	42
I. Determine sensitivity of MCNP5 results to U/Th ratio (Task 3.3) .....	43
J. Determine sensitivity of MCNP5 results to buffer thickness (Task 3.3) .....	44
K. Comments on sensitivity studies .....	45
VIII. Summary and Conclusions .....	45
IX. References .....	47
X. Students Supported by the Contract .....	49
XI. Publications Directly Related to the Contract .....	49
XII. Other Publications .....	49

## List of Figures

Figure 1.	TRISO Fuel Configurations from Microsphere to Full Core (from GA) .....	8
Figure 2.	Fort St. Vrain Reactor with Initial Fuel Loading [8] .....	12
Figure 3.	FSV control rod grouping.....	21
Figure 4.	Axial flux distribution, run 2C, region 10 (control rod out) .....	22
Figure 5.	Axial flux distribution, run 2C, region 16 (control rod in) .....	22
Figure 6.	Radial temperature zones in the FSV for MCNP5 and RELAP5 models .....	23
Figure 7.	RELAP5 axial material temperature distributions for the six radial rings .....	24
Figure 8.	MCNP5 axial normalized power distribution in fuel rings after 9 iterations .....	25
Figure 9.	MCNP5-calculated region 16 detector response as a function of boron .....	27
Figure 10.	Fitted response curve (measured data) for configuration 8, region 16 .....	28
Figure 11.	MCNP5 fitted response curves for prompt (left) and delayed (right) runs .....	28
Figure 12.	Fuel Block and Fuel Compact for FSV .....	30
Figure 13.	FSV fuel assembly (from SSP) .....	32
Figure 14.	Kernel Diameter PDFs (notional) .....	36
Figure 15.	Graphical Solution of Eq. (2) .....	38
Figure 16.	Fuel Column, Fuel Block, and Fuel Compact for FSV VHTR .....	41
Figure 17.	FSV Fuel Compact Cell .....	42

## List of Tables

Table 1.	Scope of Original Contract .....	9
Table 2.	Scope of Modified Contract .....	11
Table 3.	Initial FSV Fuel Blends .....	13
Table 4.	Number of Compacts per Blend Type .....	13
Table 5.	Fissile and Fertile Particle Data .....	14
Table 6.	TRISO Particle Sizes Used in Fort St. Vrain .....	14
Table 7.	Uranium Isotopic Composition .....	15
Table 8.	Summary of Results for Task 1 .....	16
Table 9.	MCNP5 Mass Calculation Verification .....	18
Table 10.	Best-estimate k-eigenvalues for several configurations .....	20
Table 11.	Calculated radial power distribution .....	25
Table 12.	Calculated axial power distribution .....	26
Table 13.	Configurations for the FSV pulsed neutron experiments .....	27
Table 14.	Decay constants and inferred reactivity for configuration 8 .....	29
Table 15.	Eigenvalue Sensitivity: Fuel Block Cases .....	30
Table 16.	Summary of Results for Task 2 .....	31
Table 17.	Eigenvalue results from HELIOS calculations of FSV assembly .....	32
Table 18.	Summary of Results for Task 3 .....	33
Table 19.	4-diameter Model for FSV Average Compact .....	34
Table 20.	2-diameter Model for FSV Average Compact .....	35
Table 21.	Parameters for Gaussian kernel diameter PDFs .....	38
Table 22.	Eigenvalue Sensitivity Study: 4-Particle Fuel Compact .....	40
Table 23.	Eigenvalue Sensitivity Study: 2-Particle Fuel Compact .....	40
Table 24.	Eigenvalue Sensitivity: 4-Particle Fuel Column .....	41
Table 25.	Eigenvalue Sensitivity: 2-Particle Fuel Column .....	41
Table 26.	Sensitivity to Kernel Diameter PDF for Two-Particle Model .....	42
Table 27.	Sensitivity to Kernel Diameter PDF for Four-Particle Model .....	43
Table 28.	Sensitivity to Variations in the Th:U Ratio .....	44
Table 29.	Sensitivity to Variations in the Buffer Thickness .....	44

## List of Appendices

- Appendix A. Original Proposal
- Appendix B. Request for Change in Scope and No-Cost Extension
- Appendix C. GA Trip Report and Simulation of the Fort St. Vrain Benchmark Data
- Appendix D. MCNP Fuel Loading Verification
- Appendix E. Coupled MCNP-RELAP Methodology for VHTRs
- Appendix F. Confirmation of FSV Fuel Loadings
- Appendix G. Fort St. Vrain Best Estimate Benchmark
- Appendix H. Coupled NTH Calculations for FSV (NURETH-14)
- Appendix I. Fort St. Vrain Pulsed Neutron Experiments
- Appendix J. Eigenvalue Sensitivity Studies in Support of the FSV Benchmark
- Appendix K. HELIOS Simulations of FSV Configurations
- Appendix L. Eigenvalue Sensitivity Studies in Support of the FSV Benchmark
- Appendix M. Sampling TRISO Particles for Fort St. Vrain
- Appendix N. FSV Particle Sampling Method Sensitivity Study

## Abstract

Information and measured data from the initial Fort St. Vrain (FSV) high temperature gas reactor core is used to develop a benchmark configuration to validate computational methods for analysis of a full-core, commercial HTR configuration. Large uncertainties in the geometry and composition data for the FSV fuel and core are identified, including: (1) the relative numbers of fuel particles for the four particle types, (2) the distribution of fuel kernel diameters for the four particle types, (3) the Th:U ratio in the initial FSV core, (4) and the buffer thickness for the fissile and fertile particles. Sensitivity studies were performed to assess each of these uncertainties. A number of methods were developed to assist in these studies, including: (1) the automation of MCNP5 input files for FSV using Python scripts, (2) a simple method to verify isotopic loadings in MCNP5 input files, (3) an automated procedure to conduct a coupled MCNP5-RELAP5 analysis for a full-core FSV configuration with thermal-hydraulic feedback, and (4) a methodology for sampling kernel diameters from arbitrary power law and Gaussian PDFs that preserved fuel loading and packing factor constraints. A reference FSV fuel configuration was developed based on having a single diameter kernel for each of the four particle types, preserving known uranium and thorium loadings and packing factor (58%). Three fuel models were developed, based on representing the fuel as a mixture of kernels with two diameters, four diameters, or a continuous range of diameters. The fuel particles were put into a fuel compact using either a lattice-based approach or a stochastic packing methodology from RPI, and simulated with MCNP5. The results of the sensitivity studies indicated that the uncertainties in the relative numbers and sizes of fissile and fertile kernels were not important nor were the distributions of kernel diameters within their diameter ranges. The uncertainty in the Th:U ratio in the initial FSV core was found to be important with a crude study. The uncertainty in the TRISO buffer thickness was estimated to be unimportant but the study was not conclusive. FSV fuel compacts and a regular FSV fuel element were analyzed with MCNP5 and compared with predictions using a modified version of HELIOS that is capable of analyzing TRISO fuel configurations. The HELIOS analyses were performed by SSP. The eigenvalue discrepancies between HELIOS and MCNP5 are currently on the order of 1% but these are still being evaluated. Full-core FSV configurations were developed for two initial critical configurations – a cold, clean critical loading and a critical configuration at 70% power. MCNP5 predictions are compared to experimental data and the results are mixed. Analyses were also done for the pulsed neutron experiments that were conducted by GA for the initial FSV core. MCNP5 was used to model these experiments and reasonable agreement with measured results has been observed.

## I. Introduction

The 842-MWt Fort St. Vrain (FSV) helium-cooled, graphite-moderated high-temperature gas reactor (HTR) was built by General Atomics (GA), achieved criticality in 1975, was operated from 1976-1983, and was officially decommissioned in 1989. A substantial amount of startup and operational data was obtained for the initial core and subsequent reload cores [1,2]. This data can be used to benchmark calculational methods for HTR designs that are being developed and used by various reactor analysis groups world-wide. Accordingly, the University of Michigan (UM) has pursued the development of FSV benchmark problems to allow validation and intercomparison of calculational methods and techniques for HTR analysis.

The design of the initial FSV core was intended to resemble the eventual equilibrium core for FSV, thus necessitating a wide variation in fissile/fertile loadings, with 13 different fuel blends that were distributed throughout the FSV core. In addition, the FSV fuel consisted of four different fissile and fertile TRISO kernels with different kernel diameters and coating dimensions. Figure 1 shows the complexity of a typical TRISO fuel particle and depicts fuel compacts, fuel elements, and a partial core configuration.

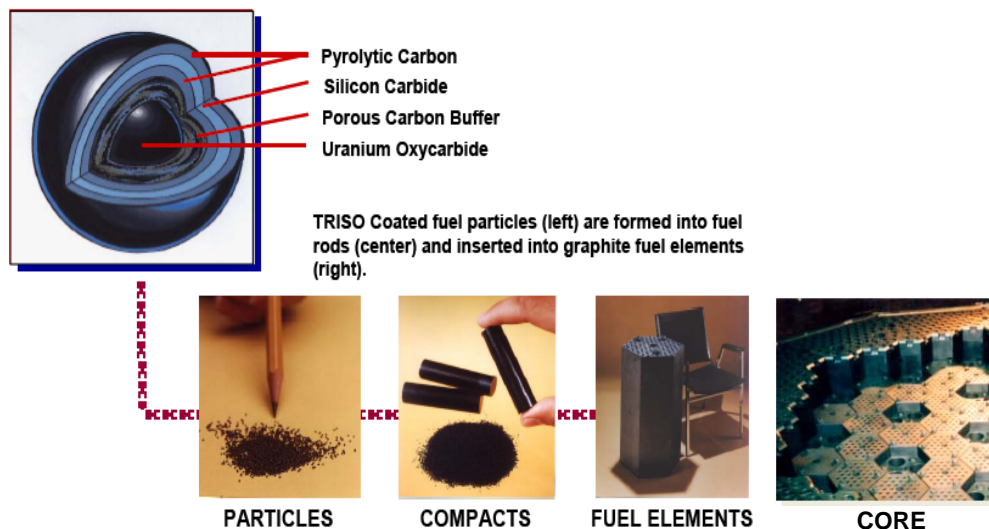


**Figure 1. TRISO Fuel Configurations from Microsphere to Full Core (from GA)**

The complexity of the FSV design and the lack of detailed fabrication records for the different types of fissile and fertile TRISO kernels forced a change in scope for this project. The details of this change in scope are discussed in the next two sections, followed by the body of the report. The report makes liberal use of previous publications and internal project reports, and these are attached as appendices.

## II. Original Project Scope

Validation of analysis methods for commercial-size reactors with experimental data has not been possible for high temperature reactors due to the lack of well-characterized full-core configurations with associated experimental measurements. The availability of a suitable full-core validation benchmark case would benefit the entire HTR analysis community by providing

precise specification of geometry and composition details as well as measured data that can be compared with predicted results, such as flux/power distributions, critical rod heights, temperature coefficients, and differential rod worths. The primary objective of this project was the development of a benchmark configuration for a commercial HTR configuration, in particular based on the FSV high temperature gas reactor. GA was a collaborating partner in this project for the development of the FSV benchmark configuration.

A secondary objective of the project was to validate an existing methodology ("Double Heterogeneity Factor" or DHF [3]) developed by the UM that allowed the analysis of arbitrary TRISO fuel configurations by a production LWR lattice physics code. The essence of the DHF method was to use explicit modeling of the TRISO fuel with the MCNP5 Monte Carlo code [4] to generate DHF correction factors that modified the resonance integrals from the lattice calculation based on a full-core Monte Carlo simulation. Studsvik-Scandpower (SSP), the owner and developer for HELIOS [5], was a collaborating partner in the effort to validate the use of DHF with HELIOS.

A tertiary objective of the project was to validate a simplified DHF methodology that did not rely on a full-core Monte Carlo simulation to calculate the DHF correction factors. SSP was also involved with this effort.

These three objectives were the basis for the three-phase project described in the original proposal (attached as Appendix A):

- Phase 1. Development and MCNP5 simulation of full-core HTR benchmark cases using data and information from the startup and operation of the FSV HTR in 1976-83. It was estimated that Phase 1 represented about 3/4 of the total project.
- Phase 2. Validation of HELIOS and the DHF method for benchmark FSV configurations with TRISO fuel. Phase 2 represented about 1/8 of the total project.
- Phase 3. Validation of the simplified DHF methodology that eliminates the need for the full-core Monte Carlo simulations. Phase 3 represented about 1/8 of the total project.

The tasks that comprised the original contract scope are shown in Table 1, along with the estimated completion dates from the original proposal.

**Table 1. Scope of Original Contract\***

#	Title	Due date
<b>1</b>	<b>Development of FSV benchmark suite</b>	<b>12/31/10</b>
1.1	Determine FSV cases	1/31/10
1.2	Obtain geometry and composition data from FSV	1/31/10
1.3	Obtain measured and operational data from GA	3/31/10
1.4	Construct preliminary MCNP5 model and compare with GA results	1/31/10
1.5	Construct benchmark MCNP5 model and compare with GA results	9/30/10
1.6	Simulation of FSV subcriticality measurements	12/31/10

<b>2</b>	<b>Validation of DHF method (Studsvik)</b>	<b>9/30/11</b>
2.1	Select FSV benchmark case	7/31/10
2.2	Run homogeneous and heterogeneous MCNP5 cases to determine DHFs	10/31/10
2.3	Run HELIOS with DHFs	9/30/11
2.4	Compare HELIOS with heterogeneous MCNP5	9/30/11
<b>3</b>	<b>Validation of simplified DHF methodology</b>	<b>9/30/11</b>
3.1	Determine DHF parameterization scheme for FSV benchmark case	12/31/10
3.2	Compare parameterized DHFs with MCNP5 DHFs	3/31/11
3.3	Run HELIOS with parameterized DHFs	9/30/11

\* Taken from 2010 Q1 Progress Report

### III. Modified Project Scope

After effort on the FSV Project had been initiated, two developments occurred that resulted in major changes to the project scope:

- HELIOS was modified by SSP to allow analysis of TRISO fuel lattices [5]. The modifications were based on the renewal theory of Sanchez [6] that allows a Method-of-Characteristics (MOC) or collision probability code to be modified to account for stochastic geometry, in particular doubly heterogeneous fuel configurations such as TRISO fuel. The feasibility of this was demonstrated in 2008 with the MOC code DeCART [7]. As a result, SSP modified their assembly transport code HELIOS to include this stochastic geometry option. This in essence made the DHF method obsolete, since the primary advantage of DHF was the ability to use a conventional LWR lattice physics code with DHF correction factors from a Monte Carlo calculation, to analyze a TRISO configuration for HTRs. Since HELIOS is an LWR lattice code and now had the capability to analyze TRISO configurations, there was no incentive to continue validation of either the DHF method or the simplified DHF method.
- There were substantial uncertainties in the geometry and composition of the TRISO fuel used in the FSV core and attempts to resolve these uncertainties, with the assistance of GA, were not successful. Due to these uncertainties, the prime objective of having a reliable benchmark configuration was at risk. The next section includes a detailed discussion of these uncertainties.

As a result of these two unanticipated developments, the following changes to the project scope were recommended by the UM (see Attachment B) and approved by DOE:

- Original Tasks 2 and 3, which pertained to the validation of the original DHF method and the simplified DHF method, respectively, were removed.
- A new task was added to redirect the HELIOS analysis to be done by SSP from a validation of DHF to a comparison (using the stochastic geometry option in HELIOS) with MCNP5 analyses for several representative TRISO configurations.
- New tasks were added to assess the the sensitivity of FSV neutronic analysis to these uncertainties by analyzing "off-nominal" cases that reflected the uncertainties in these parameters.

As a result of these scope changes, the project tasks were substantially revised. Table 2 lists the tasks in the modified contract, where blue task number indicates a modified task. As can be seen, Tasks 1.7-1.9 were added and Tasks 2 and 3 were replaced. Details on these tasks will be presented later in this report.

**Table 2. Scope of Modified Contract**

#	Title	Completion date
<b>1</b>	<b>Development of FSV benchmark suite</b>	<b>12/31/11</b>
1.1	Determine FSV cases	1/31/10
1.2	Obtain geometry and composition data from FSV	1/31/10
1.3	Obtain measured and operational data from GA	3/31/10
1.4	Construct preliminary MCNP5 model and compare with GA results	1/31/10
1.5	Construct benchmark MCNP5 model and compare with GA results	11/30/11
1.6	Simulation of FSV subcriticality measurements	11/30/11
1.7	Perform MCNP5 analysis of FSV fuel element with 2 diameter kernels	9/31/11
1.8	Perform MCNP5 analysis of FSV fuel element with 4 diameter kernels	9/31/11
1.9	Perform MCNP5 analysis of FSV fuel element with continuous diameter kernels	10/30/11
<b>2</b>	<b>Comparison of MCNP5 with HELIOS for FSV fuel elements (Studsvik)</b>	<b>11/30/11</b>
2.1	Perform HELIOS analysis of FSV fuel element with 2 diameter kernels	10/31/11
2.2	Perform HELIOS analysis of FSV fuel element with 4 diameter kernels	11/30/11
<b>3</b>	<b>Sensitivity analyses for FSV fuel parameters (fuel compacts)</b>	<b>10/31/11</b>
3.1	Perform MCNP5 analyses of fuel compacts with 2 and 4 particle types	6/30/11
3.2	Perform MCNP5 analyses of fuel compacts with continuous diameter PDFs	8/31/11
3.3	Determine sensitivity of MCNP5 results to U/Th ratio and buffer thickness	9/30/11
3.4	Determine sensitivity of MCNP5 results to relative numbers of small/large kernels	10/31/11
3.5	Determine sensitivity of MCNP5 results to choice of kernel diameter PDFs	10/31/11

# Blue task number = new task

For the remainder of this report, all references to project tasks will be based on task numbers given in Table 2.

The next section of this report describes the composition and geometry of the initial FSV core and the uncertainties that resulted in the changes to the contract scope.

## IV. FSV Fuel Parameters and Uncertainties

### A. Introduction

The composition and geometry for the FSV initial core were obtained early in the project, as described in Section V.B. This included information on startup physics tests, fuel reloading, and code calculations.

However, conflicting information was identified from other sources that led to considerable uncertainty in the initial FSV core configuration, including the dimensions and composition of the TRISO fissile and fertile particles. The effort to resolve these uncertainties was substantial and unsuccessful and led to the change in contract scope. The following paragraphs describe the sources of the uncertainties and the steps that were taken to understand and quantify them.

### B. Description of FSV Core

The FSV core has 37 fuel regions consisting of hexagonal fuel blocks with a height of 79.3 cm and a flat-to-flat distance of 36.0 cm. The active core has 247 fuel columns of six axially-stacked fuel blocks. Figure 2 depicts the initial FSV core showing the location of the fuel blends and reflector elements.

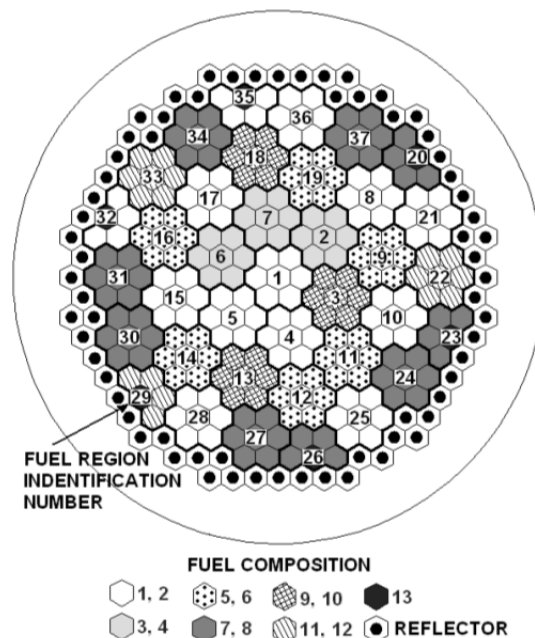


**Figure 2. Fort St. Vrain Reactor with Initial Fuel Loading**

Cylindrical fuel compacts with a radius of 0.625 cm and a height of 5.0 cm fill the fuel holes in the fuel blocks. There are 13 unique fuel blends that form the fuel compacts and each of the 13 blends consists of a specific mixture of four different TRISO particle types, corresponding to small and large diameter fertile kernels and small and large diameter fissile kernels.

The fissile kernels consist of uranium/thorium carbide fuel and the fertile kernels consist of thorium carbide fuel. Table 3 gives the uranium and thorium loadings for each of the fuel blends and Table 4 gives the number of fabricated compacts for each fuel blend [8].

**Table 3. Initial FSV Fuel Blends**

<b>Fuel Blend #</b>	<b>Uranium Mass (kg)</b>	<b>Thorium Mass (kg)</b>	<b>Fuel Blend #</b>	<b>Uranium Mass (kg)</b>	<b>Thorium Mass (kg)</b>
<b>1</b>	105.6	2905	<b>8</b>	84.4	1287
<b>2</b>	80.5	2596	<b>9</b>	36.2	720
<b>3</b>	39.2	636	<b>10</b>	25.8	599
<b>4</b>	28.9	544	<b>11</b>	32.1	549
<b>5</b>	88.8	1324	<b>12</b>	23.7	474
<b>6</b>	65.9	1158	<b>13</b>	50.5	1733
<b>7</b>	111.6	1446	<b>Total</b>	773.2	15971

**Table 4. Number of Fuel Compacts per Blend Type**

<b>Fuel Blend #</b>	<b>Number of Compacts</b>	<b>Fuel Blend #</b>	<b>Number of Compacts</b>
<b>1</b>	703098	<b>8</b>	403686
<b>2</b>	697818	<b>9</b>	185166
<b>3</b>	185166	<b>10</b>	183726
<b>4</b>	183726	<b>11</b>	135522
<b>5</b>	370332	<b>12</b>	134562
<b>6</b>	367452	<b>13</b>	367344
<b>7</b>	406566	<b>Total</b>	4324164

### **C. Description of uncertainties in the geometry and composition data**

The fissile and fertile particles differ in that the fissile kernels contain both uranium and thorium while the fertile kernels only contain thorium. Tables 5 and 6 display geometry and composition data for these particles. The key uncertainties in the fuel parameters are discussed next.

#### **1. Uncertainty in relative numbers of small and large kernels**

As a result of manufacturing tolerances and the need to have a range of particle sizes in order to achieve high packing fractions, the fissile and fertile particles were each divided into two batches: "small" and "large" diameter particles after fabrication. According to GA [9], a computer code was used to select relative numbers of particles from the "small fissile", "large fissile", "small fertile", and "large fertile" batches during fabrication of the fuel compacts in order to achieve close to a 60% packing fraction for each of the fuel blends given in Table 3. However, the resultant mixtures of small and large particles were not recorded and the computer code that was used to determine the mixtures is no longer available. GA confirmed that the relative numbers of small and large kernels were not known for either the fissile or fertile particles.

#### **2. Uncertainty in kernel diameters**

Another key uncertainty in the FSV TRISO fuel is due to the lack of data on the kernel diameters, as is evident from Table 6, where the kernel diameters are known only within

relatively large ranges. The distributions of diameters (i.e., the probability density functions or PDFs) within the listed ranges of the four particle types are unknown. Even the average kernel diameters within each range are unknown.

**Table 5. Fissile and Fertile Particle Data**

Parameter	Fissile	Fertile
Kernel Composition [8]	(Th:U)C <sub>2</sub>	ThC <sub>2</sub>
Th:U Ratio ( $\gamma$ ) [8]	3.925:1	All Th
Theoretical Density [10]	9.4 g/cc	8.96 g/cc

**Table 6. FSV TRISO Particle Geometry Data**

Dimensions ( $\mu\text{m}$ )	Fissile		Fertile	
	Small	Large	Small	Large
Kernel Diameter	100-175	175-275	300-450	450-600
Buffer Coating	50	50	50	50
Isotropic PyC Coating	20	20	20	20
SiC Coating	20	20	20	20
Isotropic PyC Coating	30	40	40	50
Total Coating Thickness	120	130	130	140

These uncertainties are a consequence of the fabrication process that yielded fuel kernels with different diameters, while the coating diameters were known reasonably well. A range of fuel particle sizes was necessary in achieving the high packing fractions in FSV compacts (~58%), but uncertainties in the kernel diameters may have a substantial impact on the neutronic analysis due to the double heterogeneity effect. The quantification of these uncertainties is one of the key goals of this project.

### 3. Uncertainty in Th/U ratio

The FSAR [10] states that a portion of the fissile fuel kernels for the initial core had a Th/U ratio of 3.6, and that this ratio was used for subsequent reload cores. However, information from other sources indicated that the Th/U ratio in the initial core was only 4.25 [9]. Subsequently GA has confirmed [9] that the initial core was a mixture of the two compositions but since the relative amounts of each were unknown, GA recommended taking an average Th/U ratio of 3.925, and this average Th/U ratio was used for this project, as indicated in Table 5. The impact of this uncertainty is discussed later in the report. The uranium is highly-enriched (93.15%), with the isotopic content given in Table 7 [11].

**Table 7. Uranium Isotopic Composition**

<b>Isotope</b>	<b>Fraction</b>
U-234	0.0078
U-235	0.9315
U-236	0.0028
U-238	0.0579

#### **4. Uncertainty in the buffer thickness**

Table 5 specifies the buffer thickness was 50 microns for both fissile and fertile particles, and was the same for small and large kernels. However, a 1994 GA report on FSV fuel experience [12] states the buffer thickness was 45-110 microns for fissile particles and 45-65 microns for fertile particles. Also, [12] states there were small differences (e.g, 5 microns) in the thicknesses of the other coatings from those given in Table 5.

Subsequently, GA [9] recommended that the values given in Table 5 should be used. The impact of the uncertainty in the fissile and fertile buffer thicknesses on the benchmark analysis was assessed and discussed later in this report.

#### **5. Uncertainty in the fabrication records**

To add assurance that the published fuel loadings in Table 3 are correct, the fabrication records for the 13 fuel blends in the initial FSV core were examined [13]. This laborious review cross-referenced the blends that went into each of the 1482 fuel blocks [14]. This review confirmed the uranium and thorium fuel loadings in Table 3, removing one source of potential uncertainty for the neutronic analysis of the initial FSV core. This effort is discussed in more detail in Section V.D.

#### **6. Change in contract scope**

These uncertainties in the FSV fuel composition and geometry led to the change in project scope that was described in Section III. The remainder of this report discusses each of the three primary tasks in the modified contract scope and the results of the studies that were carried out for each task.

### **V. Development of the FSV Benchmark Suite (Task 1)**

#### **A. Summary**

The overall goal of this task was to identify the FSV configurations that were to be the benchmark cases and collect the necessary geometry and composition data to allow simulation of these cases. Table 8 lists the sub-tasks and a short description of the results. The following discussion goes into greater detail on this task and other work that was done to support this task.

**Table 8. Summary of Results for Task 1**

#	Sub-task	Summary of Results
1.1	Determine FSV benchmark cases	Two cases were selected: (1) the initial FSV critical loading configuration at room temperature and (2) the FSV reactor at 70% power with T/H feedback.
1.2	Obtain geometry and composition data from FSV	Based on a trip to GA, discussions with GA staff, GA documents, and other sources. There were substantial uncertainties in the data as discussed in depth in Section IV.C.
1.3	Obtain measured and operational data from GA	The cases identified in Task 1.1 had measured data that has been included in this report.
1.4	Construct preliminary MCNP5 models and compare with GA results	Preliminary models were constructed for the initial FSV configuration and were reported in several quarterly reports. No further mention to this task is made in this report.
1.5	Construct benchmark MCNP5 models and compare with GA results	Results have been obtained for the two benchmark configurations identified in Task 1.1 and compared to GA data. This is discussed in Section V.G.
1.6	Simulation of FSV subcriticality measurements	Eleven subcritical FSV configurations were simulated with MCNP. This is discussed in Section V.H.
1.7	Perform MCNP5 analysis of FSV fuel element with 2 diameter kernels	All of these cases were completed and transmitted to Studsvik-Scandpower for comparison to HELIOS. This is discussed in Section V.I.
1.8	Perform MCNP5 analysis of FSV fuel element with 4 diameter kernels	
1.9	Perform MCNP5 analysis of FSV fuel element with continuous diameter kernels	

The effort to carry out the Task 1 consisted of a number of studies and analyses, some directly related to the tasks in Table 8 and other efforts that support the work on these tasks. The supporting efforts are described next and the specific effort on tasks 1.5-1.9 are described in the sections that follow.

**B. Visit to GA and preliminary FSV model**

Ben Betzler, a graduate student in Nuclear Engineering and Radiological Sciences at the UM, visited General Atomics (GA) on August 10-21, 2009. Reports acquired include information on startup physics tests, fuel reloading, and code calculations. A comprehensive report for the GA trip and the preliminary analysis of the FSV reactor based on this data was prepared by Ben Betzler and is attached as Appendix C. An ANS summary on the preliminary model was presented at the June 2010 Summer Meeting of the ANS in San Diego, CA [15]. The final

analysis of the FSV configurations will be discussed later in this report and no further mention of the preliminary analysis will be made other than drawing attention to the fact it is contained in Appendix C as well as several of the quarterly reports.

### **C. Python script to generate MCNP input files for FSV**

The modeling of full core TRISO configurations with MCNP5 results in large input files and dealing with such large input files can lead to errors, so the decision was made to create a Python [16] script that would generate the actual MCNP5 input lines based on higher level input data that describes the core composition and arrangement.

The Python script calculates average particle sizes, lattice pitches, and material compositions for all fuel blends. First, the script prompts for inputs and opens files for writing the script and any accompanying information. The inputs include level of heterogeneity and control rod insertion. The two levels of heterogeneity are heterogeneous and homogeneous fuel compacts. The heterogeneous case has a complete model of the reactor down to the individual TRISO particles. In order to preserve the proper amount of fuel in the heterogeneous case, some calculations are necessary. This calculation adjusts the TRISO packing fraction to achieve the proper amount of fuel in each compact. In this case, the script generates another file that contains information about the updated packing fraction. The homogeneous compact case smears the TRISO particles with the graphite matrix within the compacts. Control rods can either be completely inserted or completely withdrawn for either case.

After these calculations, the script writes the MCNP5 input file (may be 12,000 lines) and miscellaneous information to a separate file. The MCNP5 input file generated by Python can be directly used in MCNP5. Certain sections of the lengthy input file are repetitive, corresponding to the repeating geometry of the FSV core. Changing certain parameters in the input file often require multiple changes throughout the file. The Python script automatically edits the file when any parameters are changed: fuel loadings, packing fractions, material compositions and densities, and control rod insertion. For example, manually editing the MCNP5 input file to model control rod insertion could take hours or days and would likely lead to numerous errors but this is relatively simple with the Python script.

### **D. Automated fuel loading verification with MCNP**

The construction of the MCNP5 input file for the FSV core is challenging due to the complex composition (13 blends of fissile and fertile particles) and the complex geometry, especially when the TRISO fuel is explicitly modeled. A method has been developed that allows the user to check whether or not the correct amount of fuel is being modeled with MCNP5. Since MCNP5 cannot calculate the volume of the fuel particles if they are part of a lattice, an alternative approach was taken which involved putting a sphere around the entire FSV core and voiding all of the regions in the core but maintaining the geometry. Fictitious neutrons are then started inward isotropically on the sphere and penetrate the FSV core. Since the core is voided, the trajectories are simply straight lines through the core. The F4 tally (tracklength tally) is then used to compute the average track length in each cell, which by normalization can be shown (see Appendix D) to yield the number of particles. Folding this against the known compositions of the fuel particles yields a Monte Carlo estimate of the thorium and uranium concentrations. Using this technique for a full-core FSV calculation yielded excellent results – the MCNP5 U and Th

concentrations were all within 1% of the specified concentrations. The results of this calculation are shown in Table 9 for a full-core configuration with homogeneous fuel.

**Table 9. MCNP5 Mass Calculation Verification**

Fuel blend #	Calculated U	Actual U	Calculated Th	Actual Th
1	105.4 ± 0.2%	105.6	2900.2 ± 0.2%	2905.0
2	80.6 ± 0.2%	80.5	2598.0 ± 0.2%	2596.0
3	39.2 ± 1.2%	39.2	636.2 ± 1.2%	636.0
4	28.9 ± 1.2%	28.9	544.3 ± 1.2%	544.0
5	88.7 ± 0.4%	88.8	1321.8 ± 0.4%	1324.0
6	65.9 ± 0.4%	65.9	1158.7 ± 0.4%	1158.0
7	111.5 ± 0.3%	111.6	1445.3 ± 0.3%	1446.0
8	84.2 ± 0.3%	84.4	1283.9 ± 0.3%	1287.0
9	36.1 ± 1.1%	36.2	717.7 ± 1.1%	720.0
10	25.9 ± 1.1%	25.8	601.5 ± 1.1%	599.0
11	32.1 ± 1.2%	32.1	548.6 ± 1.2%	549.0
12	23.7 ± 1.2%	23.7	474.8 ± 1.2%	474.0
13	50.4 ± 0.5%	50.5	1731.1 ± 0.5%	1733.0

### E. Methodology for Coupled NTH Analysis using MCNP5 and RELAP5-3D

Since one of the FSV benchmark cases is the initial FSV core at 70% power, effort was directed at developing the coupled nuclear-thermal-hydraulics (NTH) methodology to couple MCNP5 and RELAP5-3D for the FSV. The reactor core was divided into 5 radial rings and 12 axial planes, with temperatures defined for each of the 60 regions. The coupled calculation starts with an MCNP5 calculation for the reactor core with an assumed temperature distribution for the 60 regions. MCNP5 computes the power produced within each region, taking into account transport of neutrons and gammas (prompt, delayed, and capture gammas), as well as point deposition of fission products and betas. Two MCNP5 runs are needed (with the PIKMT option in MCNP5 on and off) to estimate all of these fission heating contributions. An approximate model, named the ratio method, was also used which only required one MCNP5 run but is not as accurate as the PIKMT approach. A Python script post-processes the MCNP5 outputs, calculating power fractions and writing a RELAP5 input deck. RELAP5 uses these fractions to calculate temperature data. Another Python script post-processes the RELAP5 output to produce temperatures for the next MCNP5 power fraction calculation. MCNP5 input decks receive the updated temperatures, and the process repeats until convergence. A root-mean-square-deviation (RMSD) of the region temperatures is used to assess the convergence of the temperature distribution between consecutive iterations. The coupling methodology has been tested and works very well. Appendix E contains a report that describes the methodology and the test problems and results that were obtained with a coupled MCNP5/RELAP5-3D simulation of the VHTR with homogeneous fuel. A detailed discussion of the application of this NTH methodology to the FSV appears in Section V.G.2.

## **F. Confirmation of FSV fuel loadings by analyzing GA fabrication records**

The uranium and thorium loadings for the 13 fuel blends used in the initial FSV core are crucial for characterizing the FSV geometry and composition. These loadings are known from a GA document on the FSV fabrication process. Given the importance of these fuel loadings for the neutronic analysis of the FSV benchmark cases, it was decided to carry out a confirmatory analysis of the GA fuel fabrication records to verify the accuracy of the tabulated fuel loadings in the FSAR. This was a complicated analysis because the fabrication records for the 13 fuel blends in the initial FSV core [13] had to be cross-referenced with the blends that went into each of the 1482 fuel blocks [14]. The data is not in digital form and the quality of the printed report was not sufficient to allow the report to be digitally scanned and entered into a spreadsheet.

An undergraduate student was employed to examine the GA fabrication records and record in a spreadsheet the uranium and thorium loadings for each of the 1482 fuel blocks. His calculation concluded that the total number of compacts for the reactor was within .0018% of the expected value. In addition, the calculation of the total uranium weight was within .0310% of the published result and the total thorium weight was within .0218%. The number of compact calculations for all of the individual blends deviated from the expected values by less than .0034%. On the basis of this study, it was concluded that the FSV fuel loading data reported by GA is accurate and this potential source of uncertainty can be set aside. The report by Pappo is attached as Appendix F and the fabrication record spreadsheet is available by request to the project PI: W. Martin (wrm@umich.edu).

## **G. Construct benchmark MCNP5 models and compare with GA results (Task 1.5)**

There are two benchmark configurations that were analyzed by MCNP5 and compared to available measured data:

- Initial FSV critical loading configuration at room temperature (Run 2C)
- FSV reactor at 70% power with T/H feedback (Run 1H).

Table 10 is reproduced from a report on these two benchmark configurations and the pulsed neutron experiments. The report is attached as Appendix G. Figure 3 shows the FSV control rod group numbers which are keyed to the runs in Table 10. Appendix G should be consulted for details on the configurations and the cited references for the measured data.

A summary of the benchmark configurations and simulation results is given next.

### **1. Cold, clean FSV Core Configuration**

An MCNP5 model was built for Run 2C, a cold-zero-power critical configuration used for axial flux distribution measurements. The best estimate k-eigenvalue calculations yield  $1.00801 \pm .00006$ , which is a little high, especially since the MCNP5 model used homogeneous fuel. If heterogeneous fuel were to be used, this may increase another 1%, so this discrepancy indicates a problem with the input composition or geometry. Also, these results are inconsistent with the excellent MCNP5 results for Run 1H in Table 10, which used heterogeneous fuel. This issue is still under investigation.

**Table 10. Best-estimate k-eigenvalues for several configurations**

Run Id.	Control Rod Descriptions	MCNP5 <sup>1</sup>		Expected <sup>3</sup>	Measured/Experimental <sup>4</sup>	
		Heterogeneous <sup>2</sup>	Homogeneous Compact		Inhour	Area/Ratio
<b>Hot 70% Power Configurations</b>						
1H	Rod groups 3D, 4A, 4C, 4F in, rod group 3B in halfway	1.00708 ± 6	0.99731 ± 5	(Critical)	-	-
<b>Cold Core Configurations</b>						
1C	All rods in	-	0.90773 ± 19	0.902	0.904 ± 0.011	-
2C	Rod groups 1, 2A, 3C, 4B, 4F out; rod group 2B out 79.1 in	-	1.00801 ± 6	(Critical)	-	-
4C	All rods out	-	1.14072 ± 17	1.139	-	-
<b>Pulsed Neutron Configurations</b>						
4	Rod 30 out	-	0.94737 ± 20	0.944	0.940 ± 0.007	-
5	Rod 31 out	-	0.94682 ± 19	(0.944)	0.940 ± 0.007	-
6	Rod group 3C out	-	0.94517 ± 19	0.938	0.938 ± 0.007	-
7	Rod groups 3C, 2A out	-	0.98054 ± 20	0.973	0.975 ± 0.003	0.976 ± 0.003
8	Rod groups 3C, 2A, 4B out	-	0.98850 ± 19	0.981	0.983 ± 0.003	0.984 ± 0.002
9	Rod groups 3C, 2A, 4B out; rod 1 out 115 inches	-	0.99759 ± 19	0.988	0.989 ± 0.002	0.990 ± 0.001
10	Rod groups 3C, 2A, 4B, 4F out	-	0.99868 ± 19	0.991	0.992 ± 0.002	0.993 ± 0.001
11A	Rod groups 3C, 2A, 4B, 4F out; rod 1 out 112 in	-	1.00516 ± 19	(0.9975)	0.9970 ± 0.0012	0.9975 ± 0.0003
11B	Rod groups 3C, 2A, 4B, 4F out; rod 1 out 122 in	-	1.00673 ± 19	0.9975	0.9982 ± 0.0010	0.9987 ± 0.0001
12	Rods 30, 31 out	-	0.99061 ± 20	0.983	0.981 ± 0.003	0.986 ± 0.003

1 - Standard deviation error included in pcm

2 - MCNP5 only ran for 1H

3 - From GAMBLE [4] (numbers in parenthesis are estimates)

4 - From pulsed neutron experiments; 95% confidence intervals included

For Run 2C, boron-lined proportional counters were used to obtain flux measurements. These counters are sensitive to thermal neutrons. They were moved through the reserve shutdown holes in selected regions and measurements were taken at different axial heights, resulting in a measured axial thermal flux distribution. General Atomics compared GAUGE [18] calculations to the measured fluxes, with reasonable success. Furthermore, the MCNP5 models can estimate the measured thermal flux with tallies along the height of the reactor. The flux is normalized and compared to experimental and GAUGE calculated fluxes. The flux matches very well over the core region, but in the reflector region, the MCNP5 flux is significantly higher than measured. This is in part due to an inconsistency in the geometry and boron concentration of the reflector and the inputs are being corrected and rerun. This may also contribute to the over-prediction in k-eigenvalue mentioned earlier. We hope to resolve these issues during the preparation of a journal article on the simulation of FSV and comparison with measured data.

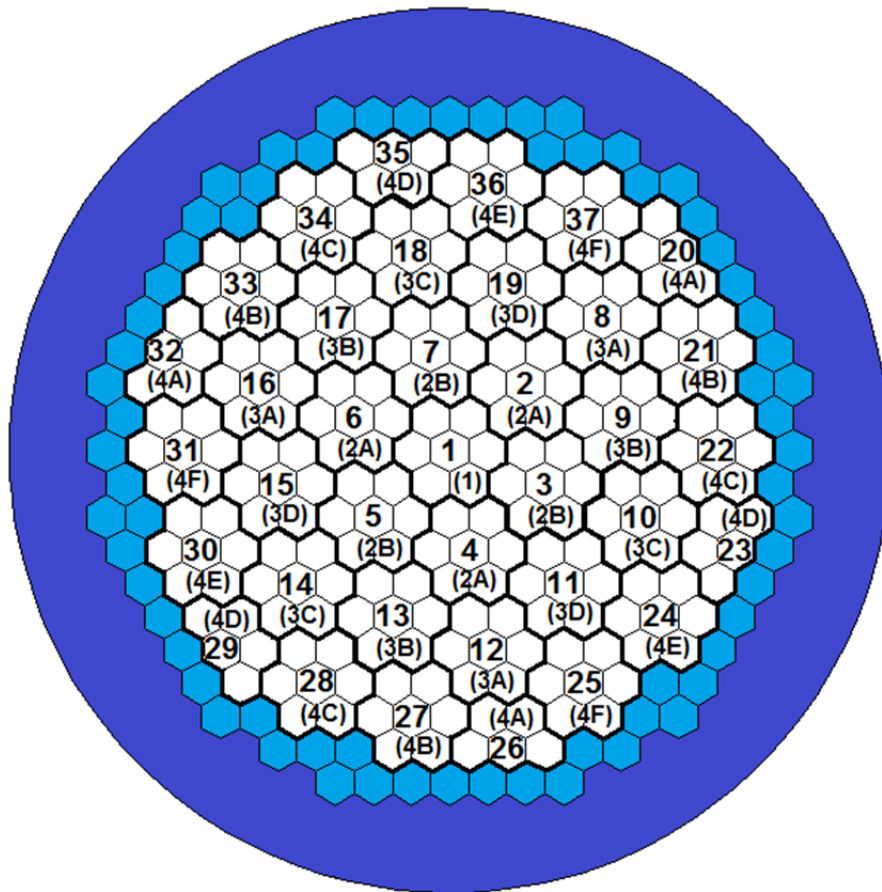


**Figure 3. FSV control rod grouping**

Although the eigenvalue comparison is suspect, the detailed flux distributions from MCNP5 show reasonable agreement with the FSV measured data. Configuration 2C was a startup experiment conducted in an air environment after initial loading [19]. Figures 4 and 5 are two representative comparisons of the MCNP5 simulation results with the FSV data. As far as small inflections and shapes of the axial flux, the MCNP5 models compare incredibly well. However, regions with or near partially inserted control rods overestimate the flux difference between the rodded and unrodded axial lengths. Furthermore, the flux recovery in the reflectors seems to be overestimated. The figures in Appendix G show all the axial flux distributions comparisons, including the GA predictions with the 3D hexagonal diffusion theory code GATT [20].

## 2. Initial FSV Core at 70% Power

The following is a summary of a coupled neutronic/thermal-hydraulic analysis of the initial FSV reactor at 70% power. This analysis is based on a paper that was presented at NURETH-14 in Toronto, Canada [21]. The full paper that was accepted for NURETH-14 has been attached as Appendix H and should be consulted for additional details on the methodology and results.

**MCNP Model.** The MCNP5 model is built to account for all the known FSV design features and technical specifications. Fuel block models account for handling holes, dowel pins, and burnable poison loadings. The model conserves the number of fuel compacts in each block [22]. For this

coupled application, a single homogenized material represents the fuel compacts; the model smears individual TRISO particles with the surrounding graphite matrix. A fully heterogeneous MCNP5 model runs in 3 to 7 days, too lengthy for this coupled setup. Results from homogeneous and heterogeneous models of the Very High Temperature Reactor (VHTR) simulations indicate that the effect of modeling the particle fuel is noticeable but not significant with respect to the converged power distribution [23].

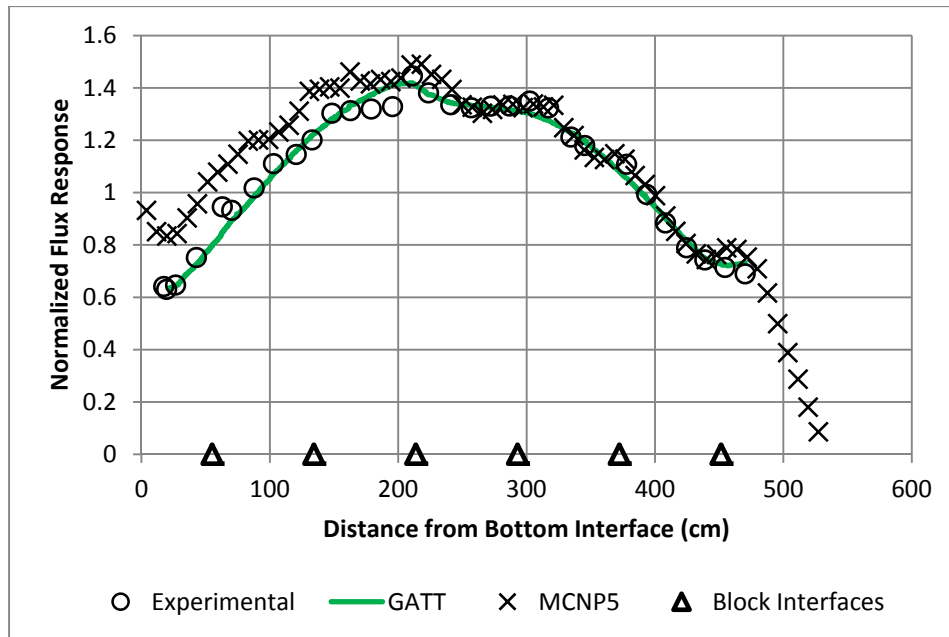


**Figure 4. Axial flux distribution, run 2C, region 10 (control rod out)**

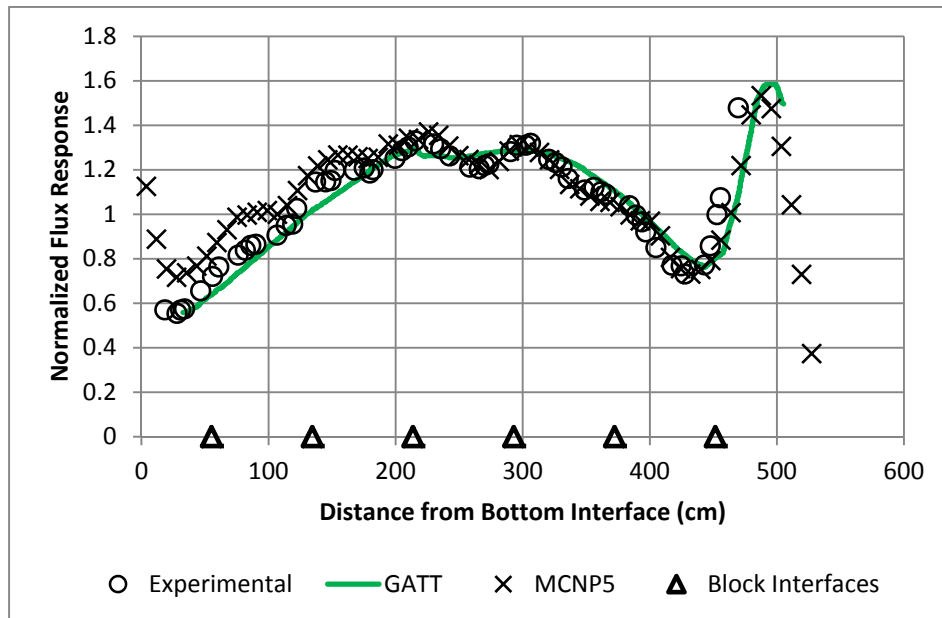


**Figure 5. Axial flux distribution, run 2C, region 16 (control rod in)**

The FSV MCNP5 model has eight axial temperature zones: six for each block of the active core and two for the top and bottom reflectors. Radially, the model has six temperature zones: four fuel regions, a replaceable reflector region, and a permanent reflector region. Figure 6 shows these radial zones. The 48 individual temperature zones and asymmetric fuel loading and temperatures push the model to the MCNP5 universe limit.

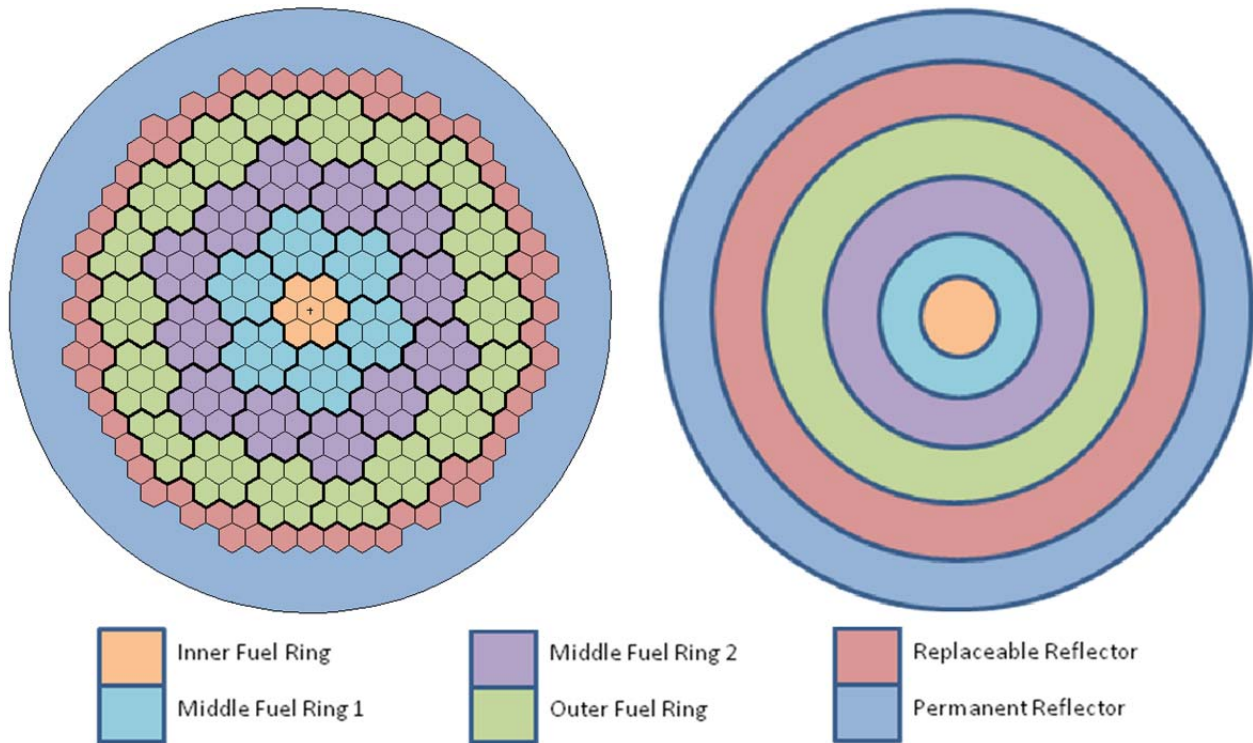


**Figure 6. Radial temperature zones in the FSV MCNP5 (left) and RELAP5 (right) models**

**RELAP5 Model.** The RELAP5 model has six radial rings with eight axial planes to reflect the FSV MCNP5 model. The four fuel rings have six axial fuel regions between top and bottom reflectors to form eight axial planes, while replaceable and permanent reflector rings have eight axial planes of graphite. Regulatory constraints limited the initial critical configuration to 70% power [24]. The RELAP5 model reflects the decreased flow and pressure corresponding to this reduced power.

Additional details on the RELAP5 model are included in Appendices E and H.

**MCNP5-RELAP5 Coupling.** A Python script post-processes the MCNP5 outputs, calculating power fractions and making a RELAP5 input deck. RELAP5 uses these fractions to calculate temperature data. Another Python script post-processes the output to produce temperatures for the next MCNP5 power fraction calculation. MCNP5 input decks receive the updated temperatures, and the process repeats until convergence, as measured by the RMSD between consecutive iterations.

**Results.** The MCNP5-RELAP5 coupled setup completed nine iterations of the PIKMT method for the initial FSV configuration. Figure 7 shows the converged axial temperature distributions in the six radial regions. Material temperature peaks at 1154K in the fourth axial plane of the first middle fuel ring. In the other three fuel rings, temperatures peak in the same axial plane at slightly lower temperatures ranging from 1085K to 1095K. The temperature gradient from the top to core centerline is greater than from the bottom to core centerline. Figure 8 shows the converged axial power distributions in the four fuel regions. The power peaks in the fourth axial plane. The top half of the core generates nearly 65% of the total power. Additional results are included in Appendix H.

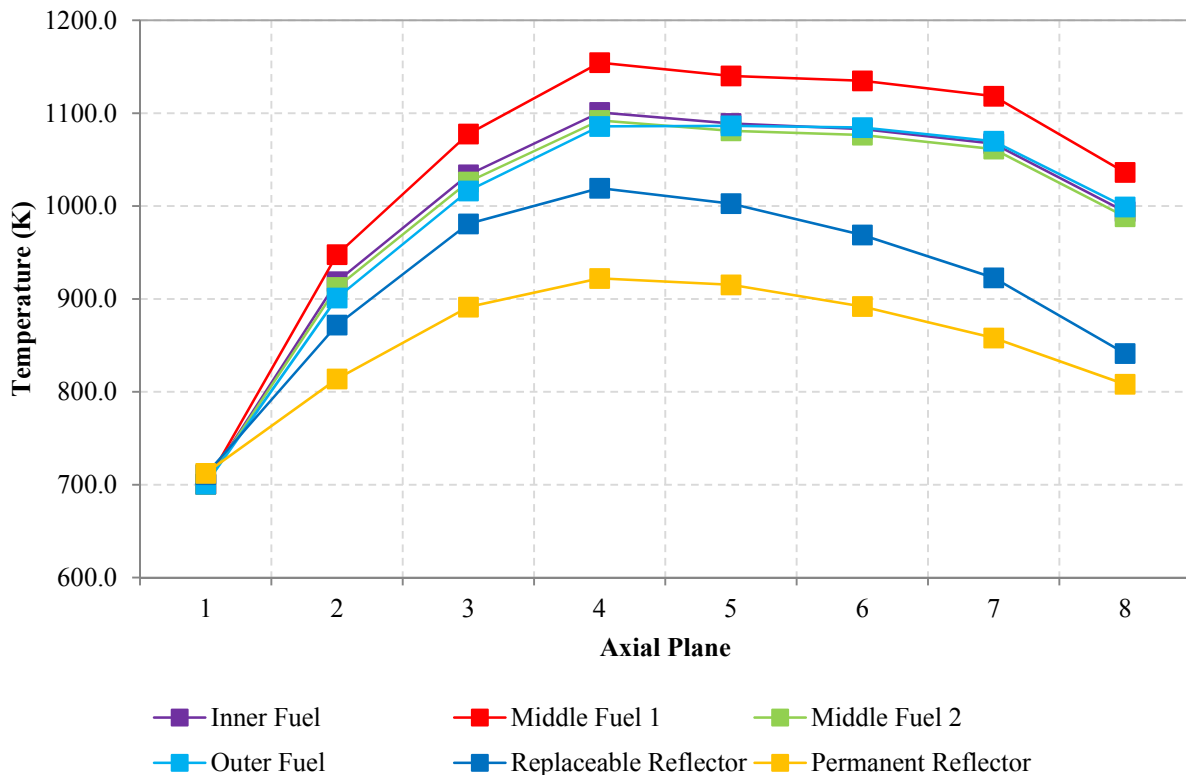


**Figure 7. RELAP5 axial material temperature distributions for the six radial rings**

**Comparison to Benchmark Results.** Due to high temperatures, FSV had no in-core instruments during operation at power. Region coolant outlet temperatures were the only online measurements. Thus, we are unable to provide a comprehensive temperature benchmark. Temperatures obtained for six axial core zones are insufficient for benchmarking, and are input to the initial MCNP5 power fraction calculation. However, calculated temperatures reflect the inlet and maximum fuel temperature.

GA used a tailored version of GATT known as GATT-2X [25] to calculate power fractions in the fuel regions of FSV for depletion studies. These fractions [26] compare well to those calculated by MCNP5. Tables 11 and 12 show the radial and axial profile comparisons, respectively. A control rod error causes the differences between the two middle rings in Table 11. Differences

for the top and bottom axial fuel planes in Table 12 likely result from a reflector geometry or density error.

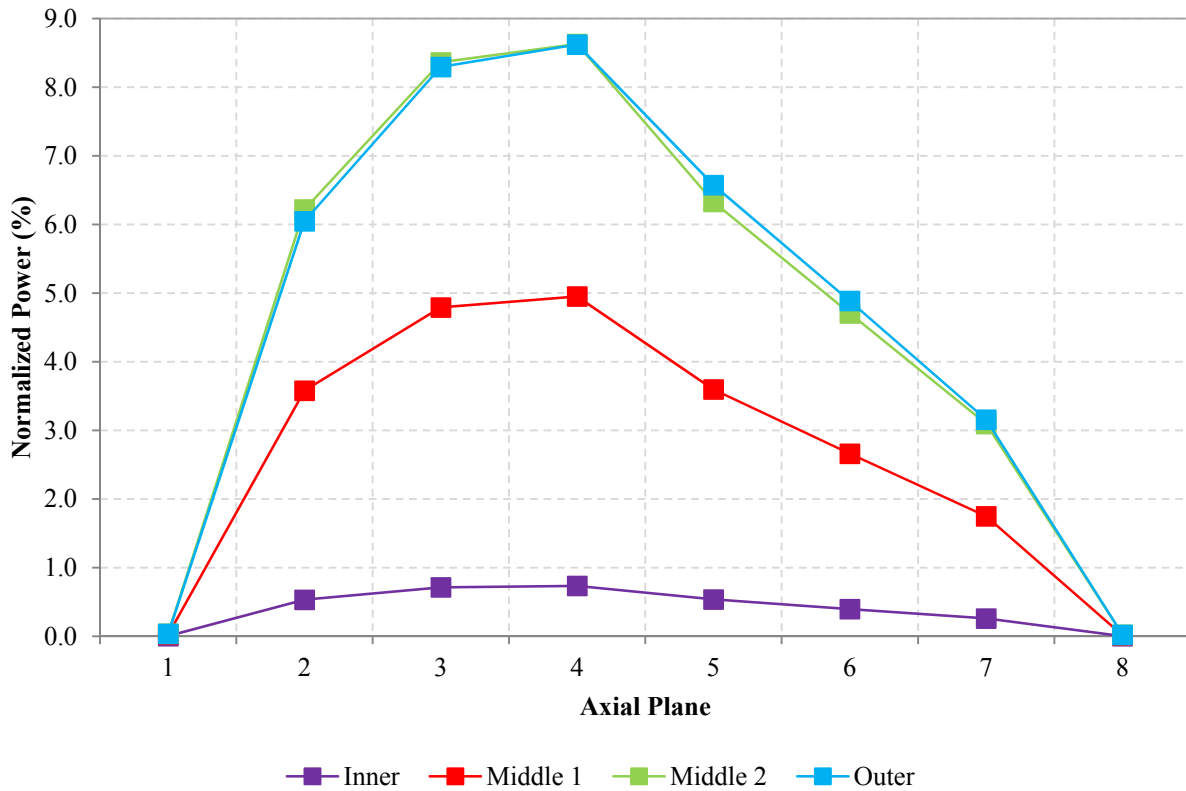


Figure 8. MCNP5 axial normalized power distribution in the fuel rings after 9 iterations

Table 11. Calculated radial power distribution

Fuel Ring	Normalized Power (%)		% Difference
	MCNP5	GATT-2X	
Inner	3.18	3.16	0.71
Middle 1	21.4	23.7	9.75
Middle 2	37.4	35.2	6.27
Outer	37.6	38.0	0.85

### H. Simulation of FSV subcriticality measurements (Task 1.6)

Pulsed neutron measurements of subcritical configurations were one of the startup neutron physics experiments slated for the FSV reactor before it went online. After loading the core, GARAN 20 experiments for 13 control rod configurations [27]. Boron-lined proportional counters connected to a multi-channel analyzer measured the local flux time response in chosen regions of FSV. With proper tallies and source definitions, MCNP5 was used to simulate these experiments. The results should be considered preliminary and have helped to assess potential inaccuracies in the MCNP5 model.

**Table 12. Calculated axial power distribution**

Axial Plane (Fuel only)	Normalized Power (%)		% Difference
	MCNP5	GATT-2X	
2	16.4	17.0	3.75
3	22.2	22.4	1.18
4	22.9	22.6	1.70
5	17.0	17.3	1.33
6	12.6	12.9	1.63
7	8.26	7.87	5.02

The following discussion summarizes the pulsed neutron experiments that were performed by GA with the initial FSV core, and describes the development of the MCNP5 model that was used to simulate the experiments. Some representative results are given below but the full report, which is attached as Appendix I, should be consulted for details on the GA experiments, the measured data, and the MCNP5 simulations.

**Pulsed neutron experiments and measured data.** After loading the initial core, FSV scientists conducted pulsed neutron experiments to measure the reactivity of given subcritical control rod configurations. A total of 20 runs were conducted for 13 control rod configurations, listed in Table 13 along with GAMBLE-calculated k-eigenvalues [28]. Figure 3 shows the control rod group numbers listed in Table 13. These experiments ran in an air environment, using mechanized drives to move sources and detectors axially within the reserve shutdown holes of the control blocks in the center of each of the 37 fuel regions. The source pulsed each configuration several times to achieve constant delayed neutron background.

**MCNP5 model.** To model these experiments with MCNP5, fuel rods are homogenized instead of modeling individual TRISO particles. Because of the presence of temporary absorbers in the first 2 configurations, only the last 11 configurations are accurately described without guesswork. The physical geometry and material composition of these temporary absorbers is unknown so these configurations were not modeled.

After obtaining measured or calculated data, it is processed to infer or calculate the reactivity, using both the area-ratio method and the inhour method. The weighted MCNP5 flux tallies are fit in much of the same manner as the measured data. However, in the MCNP5 model, the calculated detector response is only the prompt contribution from a single pulse. Therefore, the formulations are adjusted slightly. There are two treatments of delayed neutrons for the MCNP5 calculations: one with just the prompt fission contributions (with the delayed neutrons turned off in MCNP5) and one with both prompt and delayed neutron contributions.

**Comparison of Measured Data versus Calculated Results.** The MCNP5 model initially overestimated k-eigenvalue in comparison to what had been predicted or inferred by measured data. Thus, the reactivity was adjusted by increasing the boron impurity in the fuel blocks in the FSV core to 4 ppm natural boron (see Figure 9). The documented boron concentration for the FSV core fuel blocks is 1 ppm natural boron [10].

**Table 13. Configurations for the FSV pulsed neutron experiments**

Run No.	Configuration		k-eigenvalue (GAMBLE)
	No.	Description	
1	1	All temporary abosorbers in; rods 2, 4, 6 in	0.833
2, 3, 4	2, 2A, 2B	All temporary abosorbers in; rods 2, 4, 6 out	0.910
5, 6	3, 3A	All rods in	0.902
7, 8	4, 4A	Rod 30 out	0.944
9, 10	5, 5A	Rod 31 out	(0.944)
11, 12	6A, 6	Rod group 3C out	0.938
13, 14	7A, 7	Rod groups 3C, 2A out	0.973
15	8	Rod groups 3C, 2A, 4B out	0.981
16	9	Rod groups 3C, 2A, 4B out; rod 1 out 115 inches	0.988
17	10	Rod groups 3C, 2A, 4B, 4F out	0.991
18	11A	Rod groups 3C, 2A, 4B, 4F out; rod 1 out 112 inches	(0.9975)
19	11B	Rod groups 3C, 2A, 4B, 4F out; rod 1 out 122 inches	0.9975
20	12	Rods 30, 31 out	0.983

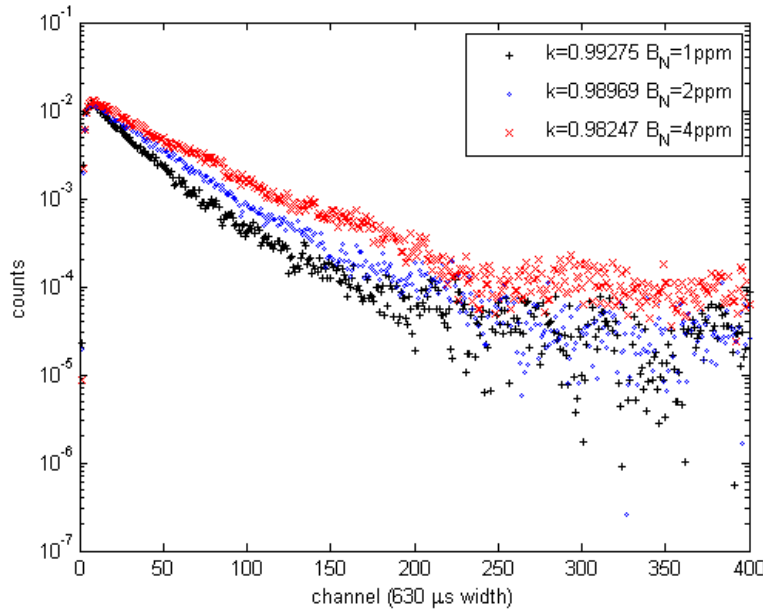


**Figure 9. MCNP5-calculated region 16 detector response as a function of boron**

The raw detector response data for configuration 8 was analyzed using the inhour and area-ratio methods that are described in Appendix I. Figure 10 shows the fitted analysis for Detector 16, where the measured counts are adjusted for the detector’s dead time losses.

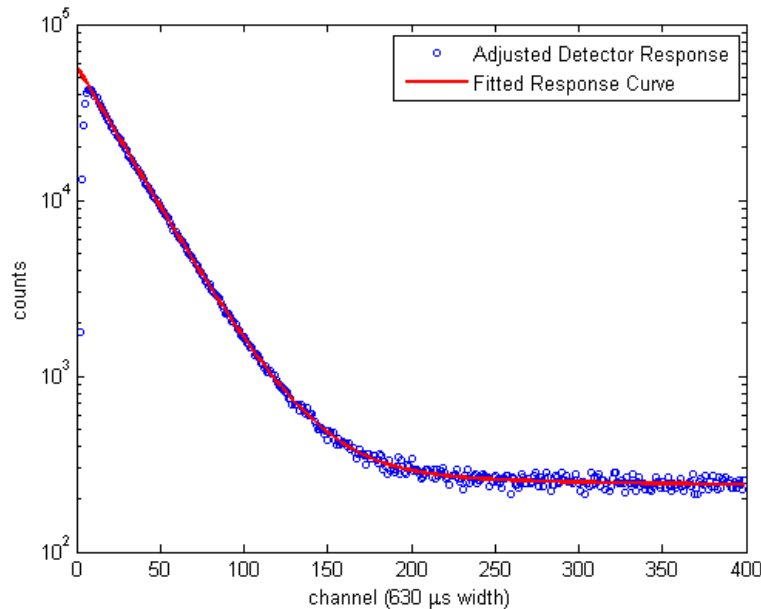


**Figure 10. Fitted response curve (measured data) for configuration 8, region 16**

This data is analyzed using similar tools for the measured data. Fitted solutions are shown in Figure 11. The exponential fit for only a single prompt mode is shown on the left. The fit uses data before channel 200. On the right is the exponential fit with delayed neutrons. The red line represents the fit to a single-pulse model, while the green line represents the delayed neutron background obtained by using the superposition concept described above. The green line shows what the detector response would look like if several hundred pulses were run. Results from this analysis are shown in Table 14 with comparison to measured data.

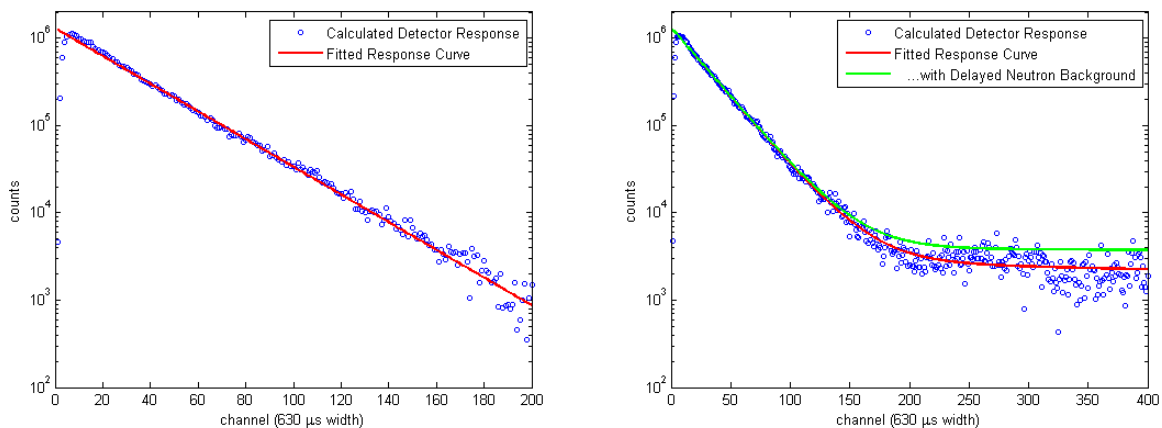


**Figure 11. MCNP5 fitted response curves for prompt (left) and delayed (right) runs**

**Table 14. Decay constants and inferred reactivity for configuration 8**

Detector Region	Extrapolated Area-Ratio Method					Inhour Method			MCNP5
	F(r)	A <sub>p</sub> /A <sub>d</sub>	ρ/β	Avg.	k <sub>eff</sub>	α	Avg.	k <sub>eff</sub>	k <sub>eff</sub>
16	1.057	3.290	-3.477	-3.206	0.980	-57.005	-56.396	0.9830	0.9825
30	0.915	3.294	-3.014			-56.355			
31	0.943	3.316	-3.127			-55.826			

The multiplication factor inferred with the inhour method shows good results for the MCNP5 tallies. However, the extrapolated area-ratio method produces more inaccurate results that may stem from spatial differences in the MCNP5 model and the FSV reactor, which would render the spatial correction factors inappropriate for the MCNP5 area-ratio calculation. This is somewhat evidenced by the relative similarity of the direct area ratios in Table 14, whereas for measured results the area ratios tend to vary more.

Still, the delayed neutron response has very poor statistics that should be increased before any solid conclusions are made. Unfortunately, the statistics obtained for later times are already near their maximum with running MCNP5 as is. The runtime used to achieve these statistics is already extremely high on several processors. A method to improve these statistics is described in Appendix I but had not been completed at the time this report was written.

**I. MCNP5 analyses of FSV fuel element (Tasks 1.7-1.9)**

The FSV fuel element was then loaded with fuel compacts loaded with 2-diameter, 4-diameter, and continuous diameter fuel kernels that are described in Section VII. Each standard fuel block consists of 3,132 compacts and reflecting boundary conditions were used radially and axially. Figure 12 shows, respectively, the fuel block and a fuel compact and shows how the compacts are placed into a block. The figures are oriented about the XZ-plane with Y = 0.9298 cm. Table 15 details the results of the eigenvalue sensitivity study.

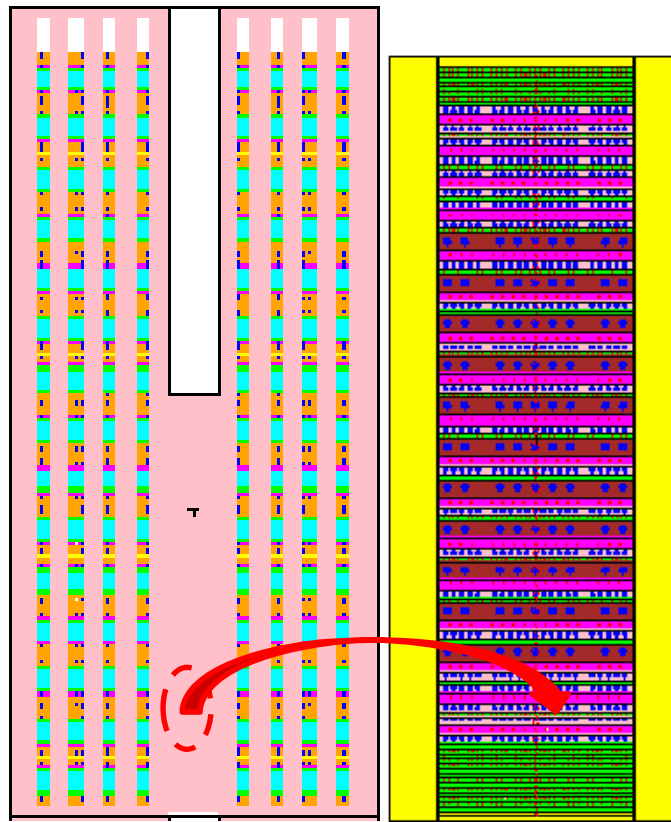


**Figure 12. Fuel Block and Fuel Compact for FSV**

Next, the 2-diameter compacts were placed into a reflecting fuel block as was done with the 4-diameter model. Table 15 presents the results of the eigenvalue sensitivity study. The standard deviations in the eigenvalues are given in parentheses (pcm).

**Table 15: Eigenvalue Sensitivity: Fuel Block Cases**

	4-particle model		2-particle model	
	Lattice-Based Method	Stochastic Method (Continuous Diameter)	Lattice-Based Method	Stochastic Method (Continuous Diameter)
k-effective	1.29010(31)	1.28744(32)	1.28985(31)	1.28719(31)
Runtime (m)	1150	14057	1211	15181

## VI. Comparison of MCNP5 with HELIOS for FSV Fuel Elements (Task 2)

### A. Summary

The overall goal of this task was to use HELIOS to analyze two FSV fuel element configurations, one with 4 different diameter kernels corresponding to small and large diameter fissile particles and small and large diameter fertile particles. This is called the discrete 4-diameter model. In addition, a discrete 2-diameter model was developed by condensing the 4-diameter model to generate single diameter fissile and fertile particles. By construction, the 2 and 4-diameter models satisfy the FSV fuel loading specifications. The UM transmitted the geometry and composition data for both models to Studsvik-Scandpower (SSP) to use HELIOS to analyze the configurations and compare with the MCNP5 simulations that were done at the UM. Table 16 lists the sub-tasks and a short description of the results that were obtained. The following discussion goes into greater detail on Task 2 and other work that was done to support this task.

**Table 16. Summary of Results for Task 2**

#	Sub-task	Summary of Results
2.1	Perform HELIOS analysis of FSV fuel element with 2-diameter kernels	Both tasks have been completed and are discussed in Sections VI.B and VI.C.
2.2	Perform HELIOS analysis of FSV fuel element with 4-diameter kernels	

SSP carried out the HELIOS simulations of both the 2-particle and 4-particle models for a FSV fuel element.

### B. HELIOS analysis and comparison with MCNP5 (Tasks 2.1 and 2.2)

The UM transmitted to SSP a report summarizing the composition and geometry specifications for the FSV fuel element which is shown in Figure 13. This report, which is attached as Appendix J, included the MCNP5 analyses performed by the UM and the corresponding MCNP5 input/output files. SSP carried out an analysis of the FSV fuel element with both 2-particle fuel and 4-particle fuel, using the HELIOS capability to analyze heterogeneous TRISO fuel with different size fuel particles. The details for the HELIOS calculations are given in Appendix K.

Two cross section libraries were used for the calculations: a 177-group library and a 335-group library. Calculations were performed for an infinite lattice of FSV fuel pin-cells (2-particle fuel model only) and for an infinite array of FSV fuel assemblies with both the 2-particle and 4-particle fuel models. The results for the FSV calculations are shown in Table 17, with the HELIOS results compared to the stochastic model MCNP results.

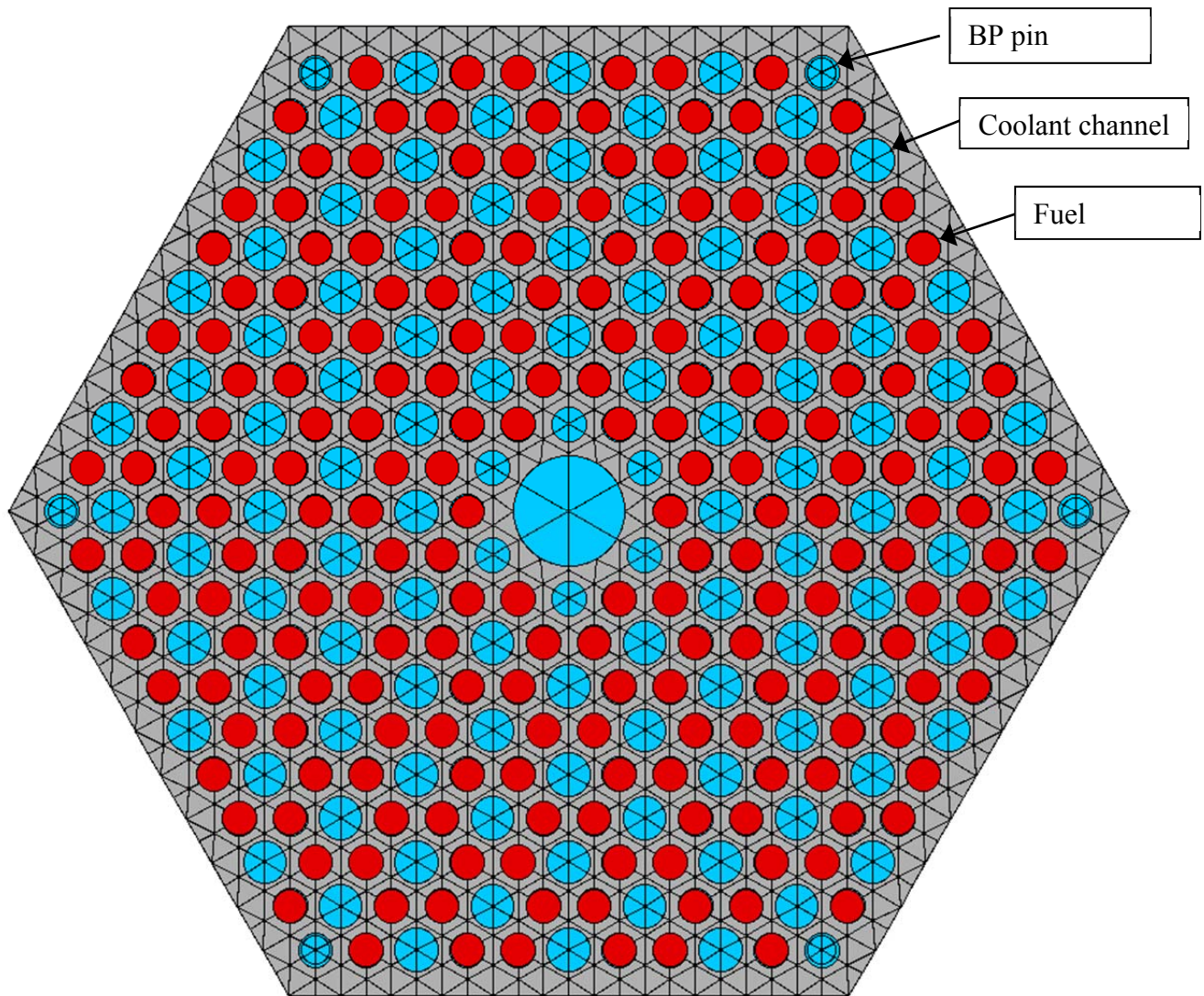


**Figure 13. FSV fuel assembly (from SSP)**

**Table 17. Eigenvalue results from HELIOS calculations of FSV assembly**

Case Description	HELIOS	MCNP	$\Delta k$ (pcm)
Pin-cell, 2-particle, 177gr library	1.14857	1.18217	3360
Pin-cell, 2-particle, 335gr library	1.14688		3529
Pin-cell, 4-particle, 177gr library	1.14728	1.18283	3555
Pin-cell, 4-particle, 335gr library	1.14558		3725
Assembly, 2-particle, 177gr library	1.24753	1.28719	3966
Assembly, 2-particle, 335gr library	1.24631		4088
Assembly, 4-particle, 177gr library	1.24637	1.28744	4107
Assembly, 4-particle, 335gr library	1.24515		4229

### C. Discussion of HELIOS and MCNP5 differences (Tasks 2.1 and 2.2)

The 3-4% difference between the HELIOS and MCNP5 eigenvalues in Table 17 indicates a failure in modeling the geometry and/or composition of the FSV fuel element with either MCNP5 or HELIOS, or both. SSP noted a few inconsistencies between the HELIOS and MCNP5 runs, including:

- Density (g/cc) of graphite block material – potential eigenvalue effect: ~1700 pcm
- Use  $S(\alpha,\beta)$  for graphite block – potential eigenvalue effect: ~250 pcm
- Inconsistency in the SiC fraction in the matrix - eigenvalue effect: ~1300 pcm.
- Use  $S(\alpha,\beta)$  for the pyrolytic carbon and matrix materials: eigenvalue effect: ~150 pcm.

These yield a total eigenvalue effect of approximately 3400 pcm, which is essentially the observed difference between the HELIOS and MCNP5 results. The UM is now examining these differences and have confirmed the density and  $S(\alpha,\beta)$  items, but are still actively examining this issue. At the time this report was written, the overall discrepancy has been reduced to ~ 1.2%. This is still too high, but much better than the 3-4% difference reported in Table 17. This is still under investigation and will be resolved for the journal publication on the FSV simulation that is in preparation.

## VII. Sensitivity Analyses for FSV Fuel Parameters (Task 3)

### A. Summary

Task 3 consisted of a number of sensitivity studies to assess the impact of the uncertainties in the FSV fuel composition and geometry. Table 18 lists the sub-tasks and a short description of the results that were obtained. The next sections describe the reference FSV fuel configuration and the results of the sensitivity studies for the sub-tasks listed in Table 18.

**Table 18. Summary of Results for Task 3**

#	Sub-task	Summary of Results
3.1	Perform MCNP5 analyses of fuel compacts with 2 and 4 particle types	Sensitivity studies were completed for fuel compacts as well as fuel columns and are discussed in Sections VII.F and VII.G.
3.2	Perform MCNP5 analyses of fuel compacts with continuous diameter PDFs	Sensitivity studies were performed with sampled kernel diameters, as discussed in Sections VII.F and VII.G.
3.3	Determine sensitivity of MCNP5 results to U/Th ratio and buffer thickness	This was completed and results indicated that the neutronic analysis was sensitive to the Th/U ratio (with constant U) but not very sensitive to the buffer thickness. These studies are discussed in Sections VII.H and VII.I, respectively.
3.4	Determine sensitivity of MCNP5 results to relative numbers of small/large kernels	This was completed and results indicated that the neutronic analysis was not very sensitive to the relative number of small/large kernels. This is discussed in Section VII.F.

## B. Development of reference 4-diameter model

Given the significant uncertainties in both composition (e.g., U/Th ratio) and geometry (e.g, the relative number of small vs. large particles and the distributions of kernel diameters), it was decided that a sensitivity analysis was needed to assess the impact of these results on the neutronic analysis. To accomplish this, a reference case was developed to assess the impact of the following uncertainties:

- Uncertainty in relative numbers of small and large fissile kernels and small and large fertile kernels (4 particle types)
- Uncertainty in the distributions of kernel diameters for the 4 particle types
- Uncertainty in the overall Th/U ratio
- Uncertainty in the buffer thickness

To obtain the reference case, an average fuel compact for the FSV was determined using the nominal fuel specifications and the "best" values for the uncertain fuel parameters. Using this average fuel compact, the uranium and thorium loadings and fuel packing fraction are constant for all of the results presented in this paper. The reference fuel configuration is the "4-diameter" model, consisting of single diameter fuel particles for each of the 4 particle types. The following summarizes the methodology to determine the reference 4-diameter system. The details are given in Attachment L.

Using the average uranium and thorium loadings, densities for the nominal compact can be found. The fuel kernel diameters for each fuel particle type are assumed to be the arithmetic averages of the kernel diameter ranges specified in Table 6. Equations for the fissile and fertile fuel densities are then combined with equation for the specified packing factor (58%) ,

$$f = \frac{4}{3} \left[ \frac{\sum_{i=s,l} N_i^{fiss} (d_i^{fiss,T})^3 + \sum_{i=s,l} N_i^{fert} (d_i^{fert,T})^3}{r_C^2 h} \right] \quad (1)$$

where N is the number of particles of a specific type,  $r_C$  is the compact radius, h is the compact height and  $d_s^{fiss,T}$ ,  $d_l^{fiss,T}$ ,  $d_s^{fert,T}$  and  $d_l^{fert,T}$  are the total (T) fuel particle diameters found by adding the kernel diameter to twice the coating thickness. This analysis results in the 4-diameter fuel compact model given in Table 19.

**Table 19. 4-diameter Model for FSV Average Compact**

	Fissile		Fertile	
	Small	Large	Small	Large
Kernel Diameter (μm)	137.5	225	375	525
Total Coating Thickness (μm)	120	130	130	140
TRISO Diameter (μm)	377.5	485	635	805
Number of Particles	54659	4637	10542	1013

### C. Equivalent 2-diameter model

An equivalent 2-diameter system was derived from the reference 4-diameter system by preserving the total uranium and fuel loadings, and the packing fraction of 58%. The purpose of this model is to have the simplest representation of the FSV core that allows separate fissile and fertile fuel particles. A note on terminology. It is usually the case in this report that "2-diameter" is equivalent to saying "2-particle" and these terms can be and are used interchangeably in this report. However, a stochastic compact with 2-particle fuel (or 4-particle fuel) may have a continuous distribution kernel diameters for each particle type. The meaning will be evident in the context of the sentence.

The number of particles for each of the two particle types is determined by reducing the 4-diameter model, but preserving fuel loadings and packing fraction. Table 20 summarizes the resultant fuel parameters used for the 2-diameter model. Note that the equivalent fissile and fertile kernels do not have realistic diameters, although the coating thicknesses are correct. The 2-diameter model was used in the sensitivity studies that are described in a following section. In addition, SSP analyzed the FSV fuel element with 2-diameter fuel with HELIOS for comparison with MCNP5, as discussed in Section VIB.

**Table 20. 2-diameter Model for FSV Average Compact**

<b>Model parameters</b>	<b>Fissile</b>	<b>Fertile</b>
Kernel Diameter (μm)	155.2	407.6
Layer Thickness (μm)	125	135
TRISO Diameter (μm)	405.2	677.6
Number of Particles	52139	10374

### D. Continuous diameter model

One of the key uncertainties in the FSV fuel geometry was the PDF for the diameters in the specified diameter ranges for each kernel type, as given in Table 6. To examine this uncertainty, a method for sampling random kernel diameters from a plausible PDF had to be developed. Since a random distribution of diameters would not be likely to satisfy the FSV fuel loading and packing factor constraints, an alternative approach to sampling the kernels was developed. The basic idea behind the method was to start with the reference 4-diameter model which was known to satisfy the fuel loading and packing factor specifications. For each of the 4 particle types, the following approach was taken to determine a suitable PDF:

- Given  $[a, b]$  as the known range of diameters from Table 6, PDFs  $f_1(D)$  and  $f_2(D)$  were postulated the small diameter range  $[a, x]$  and the large diameter range  $[x, b]$ , respectively, where  $x = (a + b) / 2$  and  $D$  is the random kernel diameter.
- $f_1(D)$  and  $f_2(D)$  were constrained to peak at  $D = x$  and go to zero at  $D = a$  or  $D = b$ , respectively. The PDFs were initially chosen to be polynomials of order 0 to 5 but one-sided Gaussians were also used.
- Determine  $P$ , where  $P =$  the probability of choosing a diameter in the range  $[a, x]$ , on the basis that the average volume (i.e., the average value of  $D^3$ ) was equal to the volume of

that kernel from the 4-diameter system. This would ensure that the fuel loadings were preserved.

- Sample kernel diameters  $D$  using the PDF  $f(x) = Pf_1(D) + (1 - P)f_2(D)$ , where  $f_1(x)$  and  $f_2(D)$  are the PDFs for  $a \leq D \leq x$  and  $x \leq D \leq b$ , respectively, and  $P$  is the probability of choosing  $D \leq x$ .
- Continue sampling kernels until the accumulated kernel volume is equal to the corresponding kernel volume for that particle type from the 4-diameter system. This will also yield statistically the same number of particles of that type.
- Determine a modified probability  $P'$  to preferentially select diameters larger than  $x$ . Since the coating volumes are not very sensitive to the kernel diameter, any kernels sampled with diameter less than  $\bar{D}$  will result in too high a coating volume, hence the packing fraction will be too high. To address this, the probability  $P$  is biased to select more larger diameter kernels than with the same PDF over the entire interval  $[a,b]$ . This can be done empirically. Later it was found by Wei Ji of RPI that the modified probability  $P'$  could be determined analytically that would preserve both kernel volume and total volume, hence preserving the packing fraction.

Figure 14 gives a visual description of the kernel diameter PDFs described above. The variables  $y_1$  and  $y_2$  are local variables for the two PDFs. A report on the kernel sampling methodology for piecewise power law PDFs is attached as Appendix M.

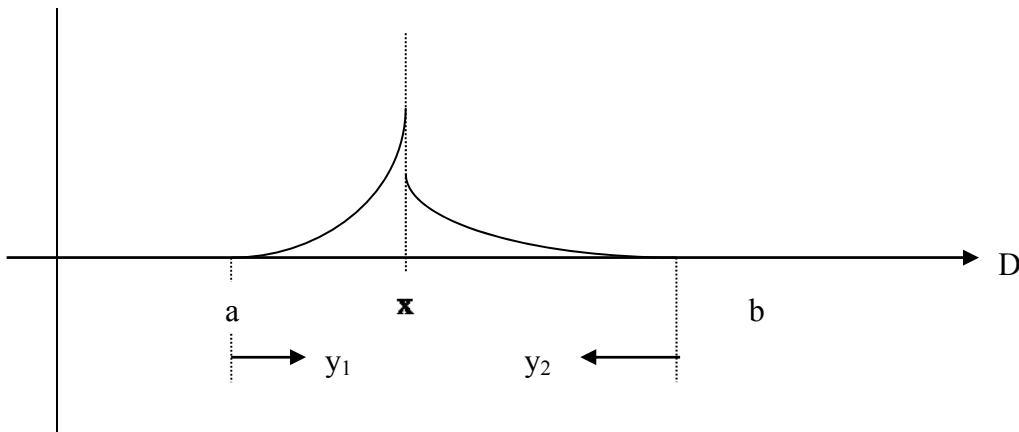


**Figure 14. Kernel Diameter PDFs (notional)**

Without the capability to sample kernel diameters and build a compact that can be analyzed by MCNP5, the FSV analysis depended on having a single diameter kernel, equivalent to a delta function PDF at  $\bar{D}$  i.e.,  $f(D) = \delta(D - x)$ . This methodology allows arbitrary piecewise power laws, including constants, over each diameter range.

This methodology was extended to a Gaussian PDF over the kernel diameter interval by an undergraduate student. He also carried out a sensitivity study for the impact of the choice of kernel diameter PDF (with both power law and Gaussian PDFs) on the neutronic analysis for the nominal FSV fuel compact. His report is attached as Appendix N. A brief summary of the

Gaussian methodology is given next but Appendix N should be consulted for details on the methodology.

A Gaussian distribution for the kernel diameters  $D$  can be expressed as follows:

$$f(D) = ke^{-\frac{(D-d)^2}{2\sigma^2}}$$

where  $k$  is the normalization factor,  $\sigma$  is the standard deviation, and  $d$  is the mean of the distribution. The factor  $k$  is needed because  $f(D)$  is clipped outside the interval  $[a,b]$ . The standard deviation is determined so that the upper and lower limits of the kernel diameter range  $[a,b]$  were two standard deviations away from the arithmetic mean, yielding  $\sigma = (b-a)/4$ , which was used for all the Gaussian PDFs. The parameter  $d$  can then be used to preserve both the kernel volume and the particle volume (kernel + coatings). This is possible because the coating thickness is known and there is a 1-1 relation between the kernel and particle volumes.

Since the Gaussian is clipped, the parameter  $d$  represents the peak of the PDF but not the mean. It biases the Gaussian PDF to preferentially sample small diameter kernels in order to preserve total particle volume.

It is shown in Appendix N that if the following equation is satisfied, the total kernel volume and total particle volume will be preserved statistically:

$$\overline{\frac{D^2}{D^3}}_{a \rightarrow b} - a = 0 \quad (2)$$

where  $\overline{\frac{D^2}{D^3}}_{a \rightarrow b} = \int_a^b f(D) [3D^2 + 6tD + 4t^2] dD$  and  $\overline{D^3} = \int_a^b f(D) D^3 dD$ . These quantities are related to the average coating volume and average kernel volume, respectively.

Since  $f(D)$  is a Gaussian, Eq. (2) cannot be solved analytically. Instead, Eq. (2) was solved graphically. Figure 15 illustrates the graphical solution for the fertile particle in a 2-particle model. The intersection of the graph with the x-axis returns the value of  $d$  that conserves both fuel volume and packing fraction.

The clipped Gaussian has to be normalized over the interval  $[a,b]$ , yielding

$$k = -\frac{4\sqrt{\frac{2}{\pi}}}{(a-b) \left( \text{Erf} \left[ \frac{2\sqrt{2}(a-d)}{a-b} \right] - \text{Erf} \left[ \frac{2\sqrt{2}(b-d)}{a-b} \right] \right)} \quad (3)$$

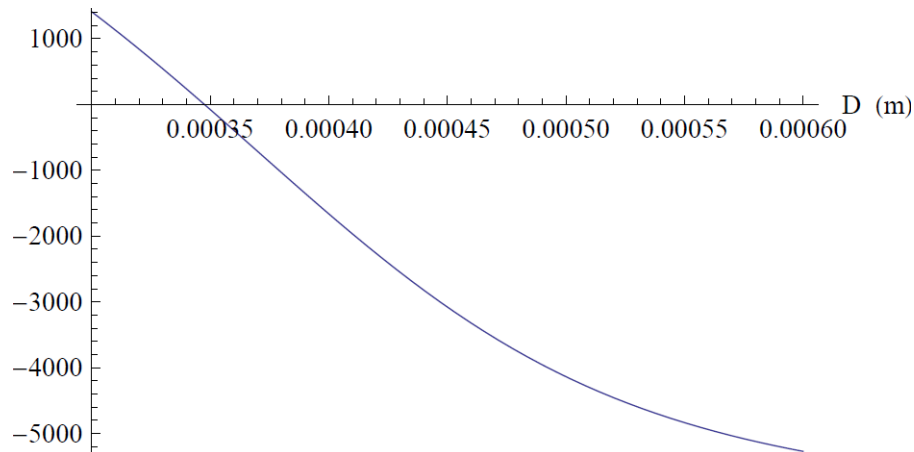


**Figure 15. Graphical Solution of Eq. (2)**

Solving the above equations for the fissile and fertile particles (two-particle model) results in the parameters given in Table 21. Note how  $d$ , the peak of the Gaussian PDF, is strongly biased towards the low end of the kernel diameter interval  $[a,b]$ .

**Table 21. Parameters for Gaussian kernel diameter PDFs**

Parameter	Fissile	Fertile
a	100	300
b	275	600
$\sigma$	43.75	75
d	113.6	347.6
k	0.0147	0.00722

### E. Stochastic compact model

It is not possible to put random diameter spheres on a lattice and expect to have a high packing fraction. More importantly, this cannot be done with MCNP5 without hand tailoring the lattice, and the packing fraction would still be too low. Therefore, it was necessary to turn to a randomly packed mixture where the spheres have random diameters from the above sampling scheme and MCNP5 simulates the actual stochastic configuration using the coordinates of each of the particles in the mixture.

The stochastic fuel compact model is based on methodology developed by Li and Ji at Rensselaer Polytechnic Institute [29]. This methodology, which was originally developed to pack spheres in a pebble bed reactor while accounting for interparticle forces such as friction and wall forces, was adapted to pack TRISO fuel particles in a cylindrical fuel compact. The methodology packs kernels up to a 60% packing fraction with its unique “settling” approach, where interparticle forces and wall forces allow an initial overlapping particle distribution to approach a realistic distribution that has no overlap and is entirely within the container, which is a finite cylinder for a fuel compact. It also has the capability to pack a fuel compact with different sized particles including those with a continuous distribution of kernel diameters sampled from PDFs, such as described in Sections VII.D and VII.H.

This particle packing methodology also writes out MCNP5 input files corresponding to the random mixture of particles. Therefore, it is possible to generate discrete diameter stochastic fuel compacts that correspond to either the lattice-based 4-particle or 2-particle fuel compacts. In addition, these models can be compared against a stochastic fuel compact consisting of particles with kernels sampled from continuous PDFs. For the stochastic fuel compacts, the 4- and 2-diameter models have the dimensions given in Tables 19 and 20, respectively. The continuous 4- and 2-diameter models sample kernel diameters from the ranges given in Table 6 using a methodology that preserves fuel loadings and packing fraction.

Stochastic FSV fuel compact configurations were modeled and run with MCNP5. The MCNP5 results for the 4-particle and 2-particle fuel compact models are compared to the stochastic fuel compact model and are discussed in the following sections.

#### **F. Results of sensitivity studies for fuel compacts (Tasks 3.1, 3.2, and 3.4)**

To study the effect of these uncertainties, both lattice-based and stochastic fuel compact models were developed, based on the reference 4-diameter model. These different configurations are summarized as follows:

- Lattice-based 4-diameter fuel compact – the reference configuration with a specified number of fixed-diameter kernels for each of the 4 fuel types corresponding to the small fissile, large fissile, small fertile and large fertile kernels, arranged in a regular hexagonal honeycomb lattice. This is equivalent to selecting a delta function PDF at the (arithmetic) average diameter for each fuel kernel type given in Table 6. Three physical arrangements of the fuel compact lattice were simulated to assess the sensitivity of the neutronic analysis to the geometry.
- Lattice-based 2-diameter fuel compact – this model is a condensation of the 4-diameter fuel compact to two different diameter particles, one for fissile fuel and one for fertile fuel, with the same regular lattice structure. The same three physical arrangements were considered as with the 4-diameter case.
- Stochastic fuel compact (2, 4, and continuous diameter kernels) – the fuel compact is modeled either as a stochastic mixture of either the 4-diameter fuel, the 2-diameter fuel, or the continuous diameter fuel. Every particle in the stochastic mixture is explicitly modeled by MCNP5, using the input files generated by the random packing code described in Section V.E. The stochastic model with continuous kernel diameters was chosen to be the benchmark calculation for comparison with the other cases since it is most representative of the physical fuel compact.

The MCNP5 results for the 4-diameter and 2-diameter fuel compacts are compared to MCNP5 calculations for stochastic fuel compacts. The stochastic model with a continuous treatment of kernel diameters is chosen as a reference, since this best represents the physical problem. The methodology for the stochastic model is described in Section VII.E.

The 4-diameter comparisons are summarized in Table 22 and show the eigenvalue sensitivity to lattice-based and stochastic models. Table 23 gives the 2-diameter results. All runs used 10,000 source histories per cycle with 400 active cycles.

**Table 22. Eigenvalue Sensitivity Study: 4-Particle Fuel Compact**

	Lattice-based			Stochastic	
	Arr. 1	Arr. 2	Arr. 3	Discrete	Continuous
k-effective	1.17463	1.17543	1.16690	1.17102	1.17010
$\sigma$ [pcm]	31	32	34	33	33
Deviation from Reference [pcm]	453	533	-320	92	---
Computer Time [hrs]	10.9	10.8	11.0	282	281

**Table 23. Eigenvalue Sensitivity Study: 2-Particle Fuel Compact**

	Lattice-based			Stochastic	
	Arr. 1	Arr. 2	Arr. 3	Discrete	Continuous
k-effective	1.17131	1.17311	1.16985	1.17013	1.17001
$\sigma$ [pcm]	32	31	32	33	32
Deviation from Reference [pcm]	130	310	-16	12	---
Computer Time [hrs]	11	11	11	249	289

The eigenvalues agree reasonably well with each other and the lattice-based compacts take far less time to run than the stochastic compacts, as expected. Lattice-based arrangement 3 agrees best with the stochastic models. Since each compact has reflecting boundary conditions, lattice-based arrangement 2 can be thought of as a translation of lattice-based arrangement 1 with a thin layer of graphite between large fertile layers. The primary observation is that the 2 and 4-particle results are not that far apart but they differ substantially in the number of particles and the sizes of the particles. This indicates that the effect of the uncertainty in the number of small versus large particles may not be that important. It was also shown earlier that the distribution of kernel diameters within the diameter range indicated for a given particle type is not an important factor, so the apparently large uncertainties in the relative numbers and sizes of the 4 particle types are not that important.

**G. Results of sensitivity studies for fuel columns**

It was decided to repeat the sensitivity studies for fuel columns consisting of the same lattice-based and stochastic compacts examined in Section VII.F. Although this was not proposed as part of the modified contract scope, it was thought this study would give additional evidence regarding the sensitivity of the neutronic results to the fuel parameters. Each fuel column consists of six fuel blocks stacked on top of one another. Each standard fuel block consists of 3,132 compacts for a total of 18,792 compacts per fuel column.

Figure 16 shows, from left to right, the fuel column, fuel block, and a fuel compact, and shows how the compacts are placed into a fuel block. The figures are oriented about the XZ-plane with the Y cross section taken along a row of fuel holes.

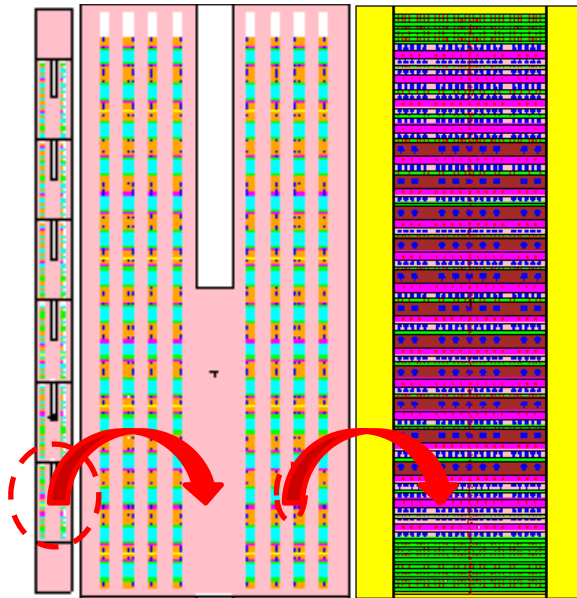


**Figure 16. Fuel Column, Fuel Block, and Fuel Compact for FSV VHTR**

Since there are three arrangements for a compact, three lattice-based fuel columns are simulated, each with a different compact arrangement. Tables 24 and 25 contain the results of the eigenvalue sensitivity studies for 4-diameter and 2-diameter fuel, respectively. The k-eigenvalues increase significantly due to the presence of added graphite in the fuel blocks and therefore a decrease in the total percentage of absorbing materials, however the trends are similar to the fuel element case and the same conclusions regarding the sensitivities to relative numbers and sizes of particles are the same.

**Table 24. Eigenvalue Sensitivity: 4-Particle Fuel Column**

	Lattice-based Method			Stochastic Method	
	Arr. 1	Arr. 2	Arr. 3	Discrete	Continuous
k-effective	1.26067	1.26316	1.25800	1.25912	1.25782
$\sigma$ [pcm]	31	32	31	31	31
Deviation from Reference [pcm]	285	534	18	130	---
Computer Time [hrs]	20.52	19.37	20.44	259.92	253.63

**Table 25. Eigenvalue Sensitivity: 2-Particle Fuel Column**

	Lattice-based Method			Stochastic Method	
	Arr. 1	Arr. 2	Arr. 3	Discrete	Continuous
k-effective	1.25927	1.26199	1.26101	1.25804	1.25832
$\sigma$ [pcm]	34	32	31	30	32
Deviation from Reference [pcm]	95	367	269	-28	---
Computer Time [hrs]	20.39	21.48	21.54	190.26	248.47

**H. Determine sensitivity of MCNP5 results to kernel diameter PDF (Task 3.2)**

Section VII.F presented results of sensitivity studies of FSV fuel configurations with 2-diameter fuel, 4-particle fuel, and continuous diameter fuel. The continuous diameter fuel model was based on a piecewise quadratic PDF as described in Section VII.D. This section examines the sensitivity of the neutronic analysis to the choice of the continuous kernel diameter PDFs, since there is no information regarding the distribution of kernel diameters within the diameter ranges given in Table 6. Section VII.D described the methodology to determine suitable kernel diameter PDFs that preserved the fuel loading and packing factor constraints for the FSV fuel particle types. This section summarizes the sensitivity studies that were carried out to determine the effect of different PDFs on  $k_{eff}$  for a FSV fuel compact cell, which is an equivalent cell that consists of a fuel compact surrounded by its share of the graphite in a regular FSV fuel element. The compact cell is shown in Figure 17.

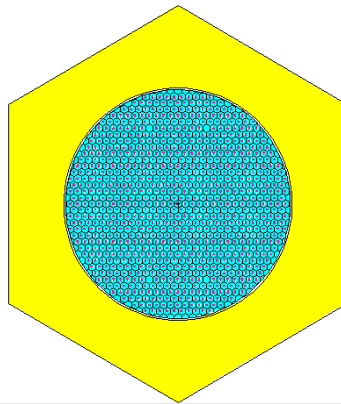


**Figure 17. FSV Fuel Compact Cell**

The PDFs that were included in the sensitivity study were piecewise continuous power law PDFs ranging from piecewise constants to piecewise quartics and the (continuous) clipped Gaussian PDFs. Both two-particle and four-particle fuel models were included in the study and the results are given in Table 26 and 27. The reference results are the quadratic piecewise PDFs.

**Table 26. Sensitivity to Kernel Diameter PDF for Two-Particle Model**

PDF	$k_{eff}$	$\sigma$ (pcm)	Difference (pcm)
Constant	1.18373	33	81
Linear	1.18285	32	-7
Quadratic	1.18292	33	0
Cubic	1.18237	32	-55
Quartic	1.18314	33	22
Gaussian	1.18286	34	-6

**Table 27. Sensitivity to Kernel Diameter PDF for Four-Particle Model**

PDF	$k_{\text{eff}}$	$\sigma$ (pcm)	Difference (pcm)
Constant	1.18311	32	43
Linear	1.18275	32	7
Quadratic	1.18268	33	0
Cubic	1.18275	33	7
Quartic	1.18314	30	46
Gaussian	1.18218	32	-50

Overall, the two-particle model eigenvalues resulting from the linear, quartic, and Gaussian PDFs were all in agreement with the eigenvalue obtained from the quadratic PDF. While the two-particle eigenvalues resulting from the constant and cubic PDFs differed more from the quadratic PDF eigenvalue, they were still within two standard deviations of the difference in the measurements. For the four particle model, the constant, linear, and cubic PDF eigenvalues were within one standard deviation of the quadratic PDF eigenvalue, while the quartic and Gaussian PDF eigenvalues were within two standard deviations of the quadratic PDF eigenvalues. Therefore, the majority of difference between the results is from statistical uncertainty, not from a difference in the true eigenvalues. As a result, it is concluded that the eigenvalue is insensitive to the PDFs used to sample the kernel diameters.

**I. Determine sensitivity of MCNP5 results to U/Th ratio (Task 3.3)**

Task 3.3 was a sensitivity study to assess the effect of uncertainties in both the Th:U ratio and the buffer thickness. This section treats the Th:U ratio study and the next section discusses the buffer thickness study.

As noted in Section IV.C.3, the initial FSV core is a mixture of fissile fuel batches with Th/U ratios of 3.6 and 4.25 and the relative amounts of each is not known. We have chosen to use a Th/U ratio of 3.925, which is simply the average ratio assuming a 50-50 mixture. In order to assess the uncertainty of this parameter, the 2-diameter and 4-diameter fuel compacts were modified to have Th/U ratios of 3.6 and 4.25, and these compact cells were then compared to the average compact cell with Th/U ration of 3.925.

When the fissile Th:U ratio is changed, the mass of fissile thorium changes as well as the number of each type of fissile and fertile kernels. Since this would complicate the comparison because a number of other factors are changing, it was decided to simplify the perturbation by preserving the number and size of fissile and fertile particles. Instead, the Th:U ratio in the fissile particles would be changed by altering only the thorium number density, thus keeping the uranium density constant. Since the total thorium loading is specified, the thorium density in the fertile particles is then modified to preserve the average thorium loading in the fuel. This results in a fuel with identical geometry but altered thorium densities in the fissile and fertile particles, preserving both total uranium and total thorium for the average compact, as well as the 58% packing factor. This latter parameter is important to preserve because it was well-characterized by GA during fabrication of the FSV fuel. Any changes to the geometry would have modified the packing factor, and this would have entailed a more complicated study.

Since the geometry was the same, the lattice-based 2 and 4-diameter models can be used to analyze the perturbed cases, since only the thorium densities have changed. The sensitivity calculations were made with lattice-based arrangement and the results are given in Table 28, where  $\gamma$  is the Th:U ratio in the fissile fuel kernel.

**Table 28. Sensitivity to Variations in the Th:U Ratio**

	$\gamma = 3.6$	$\gamma = 3.925$	$\gamma = 4.25$
<b>2-diameter</b>	1.18565(31)	1.16985(32)	1.15431(32)
<b>4-diameter</b>	1.18371(32)	1.16690(34)	1.15184(33)

As the fissile Th:U ratio increases, the eigenvalue decreases for two and four-diameter models. An increase in ratio of 0.325 causes a decrease in eigenvalue by about 1500-1600 pcm. This trend makes sense because the amount of thorium increases with the Th:U ratio, thus decreasing the reactivity of the fuel, causing  $k_{eff}$  to decrease.

It can be seen from Table 28 that the reactivity effect of the uncertainty in the Th:U ratio is significant, at least for the fuel compact cell when only the thorium content is changed as was done here. To properly investigate this uncertainty, it may be necessary to generate full-core FSV configurations that consist of fuel elements with Th:U ratios of both 3.6 and 4.25, consisting of fuel compacts with thorium and uranium densities that realistically reflect these ratios and maintaining the overall fuel loading and packing factor constraints. This will necessitate generation of new 2 and 4-particle systems similar to what was done in Section VII.B for the average Th:U ratio. This is likely to be a substantial effort but may be warranted due to the significant effect the Th:U ratio has on the eigenvalue.

**J. Determine sensitivity of MCNP5 results to buffer thickness (Task 3.3)**

This section discussed the portion of Task 3.3 related to the assessment of the uncertainty in the buffer thickness. A thorough study of this uncertainty would require regeneration of the reference 4-particle and 2-particle models, because the buffer thickness affects the packing fraction. A simpler approach was taken to gauge the effect of a small change in the buffer thickness to get a sense for the impact on the neutronic analysis.

Both the 2-diameter and 4-diameter lattice-based models were analyzed. Similar to the reasons given in the previous section, the packing factor was kept the same by keeping the geometry constant and changing the buffer density by  $\pm 10\%$ . Since the coatings are homogenized into the matrix region surrounding the particles, this is tantamount to a change in the buffer thickness, holding everything else constant. The results of the MCNP5 simulations are given in Table 29.

**Table 29. Sensitivity to Variations in the Buffer Thickness (Density)**

	$\rho = 1.0$	$\rho = 0.9$	$\Delta k$ (pcm)	$\rho = 1.1$	$\Delta k$ (pcm)
<b>2-diameter</b>	1.16921	1.16943	22	1.16944	23
<b>4-diameter</b>	1.16690	1.16668	22	1.16812	131

The standard deviation for all eigenvalues was less than 35 pcm and the differences are with respect to the nominal buffer density for each fuel model. The 4-diameter result for the increased

buffer density is inconsistent with the other results and is likely due to an error in the analysis. All of the other results show differences that are less than the standard deviation in the eigenvalue ( $< 35$  pcm for all cases), so this indicates that the uncertainty in the buffer thickness may not be significant.

It would be better to conduct a more thorough analysis of the buffer thickness effect. The simple approach taken is tantamount to assuming that every particle in the fuel compact has the same buffer thickness, whether nominal or perturbed, while in reality the fuel compact will consist of particles with a distribution of buffer thicknesses. A better approach would be to modify the sampling methodology for kernel diameters described in Section V.II to sample buffer thicknesses while preserving packing fraction. This would be a straightforward extension of the sampling methodology. Together with the stochastic compact model in Section VII.E, this would allow an MCNP5 simulation of a stochastic fuel compact with a random distribution of buffer thicknesses but with the same fuel loadings and packing fraction. This would be a definitive sensitivity study for the uncertainty in the buffer thickness but could not be done in time for this report.

#### **K. Comments on sensitivity studies**

Appendix J contains an internal report on many of the sensitivity studies discussed in this section. In addition, [31] discusses the FSV sensitivity studies and was presented at PHYSOR-2012 in Knoxville, TN in April 2012.

Although fuel composition and fabrication data were provided, there are substantial uncertainties in several of the key fuel parameters. Most of these do not impact the neutronic analysis significantly, including the unknown distributions of kernel diameters, the relative number of small versus large kernels for either fissile or fertile particles, and the thickness of the buffer coating. The uncertainty in the Th:U ratio was important but was difficult to quantify in a sensitivity study involving only fuel compacts. The uncertainty in the buffer thickness appeared to be modest but there are some questions regarding the analysis. Better methods for assessing the uncertainties in the Th:U ratio and buffer thickness are suggested.

### **VIII. Summary and Conclusions**

The primary objective of this project was to use information and measured data from the initial FSV core to develop a benchmark case for a full-core, commercial HTR configuration. This benchmark case would then be used to validate the DHF methodology developed by the UM that allowed the analysis of arbitrary TRISO fuel configurations by a production LWR lattice physics code. In addition, a simplified DHF methodology would also be validated.

These objectives were challenged by large uncertainties that were identified as the geometry and composition data for the FSV fuel was collected. In addition, modifications were made to the HELIOS code to allow it to analyze TRISO fuel configurations, removing the incentive to validate the DHF methodology. As a result, the scope of the contract was modified to remove the DHF efforts and focus the effort to understanding and quantifying the uncertainties in the FSV fuel design and initial core loading.

The key uncertainties were identified to be: (1) the relative numbers of fuel particles for the four particle types, (2) the distribution of fuel kernel diameters for the four particle types, (3) the Th:U ratio in the initial FSV core, (4) and the buffer thickness for the fissile and fertile particles.

Sensitivity studies were performed to assess each of these uncertainties. A number of methods were developed to assist in these studies, including: (1) the automation of MCNP5 input files for FSV using Python scripts, (2) a simple method to verify isotopic loadings in MCNP5 input files, (3) an automated procedure to conduct a coupled MCNP5-RELAP5 analysis for a full-core FSV configuration with thermal-hydraulic feedback, and (4) a methodology for sampling kernel diameters from arbitrary power law and Gaussian PDFs that preserved fuel loading and packing factor constraints.

To carry out the sensitivity studies, a reference FSV fuel configuration was developed. This reference configuration was based on having a single diameter kernel for each of the four particle types, and that preserved the known uranium and thorium loadings for this particle type and the packing factor (58%). This reference configuration is denoted the "4-diameter" or "4-particle" model. A "2-particle" model was derived from the "4-particle" model and this also preserved the uranium and thorium loadings and the packing factor. A "continuous diameter" model was also developed for each of the "4-particle" models by developing a sampling scheme to sample kernel diameters that preserved the fuel loading and packing factor from the "4-particle" model. These sampled fuel particles were packed into a fuel compact using a stochastic packing methodology from RPI and simulated with MCNP5. This stochastic packing method was also used to construct stochastic fuel compacts of "4-diameter", "2-diameter", and "continuous diameter" fuel particles.

The results of the sensitivity studies indicated that the uncertainties in the relative numbers and sizes of fissile and fertile kernels were not important, when the uranium and thorium loadings and packing factors were preserved. In addition, the distributions of kernel diameters within their diameter ranges were not important. The fact that these uncertainties did not have a significant impact on the neutronic analysis was not expected. Perhaps the most important uncertainty was the Th:U ratio. A simple sensitivity study indicated this was an important quantity but this was not quantified because this would have required a much larger study than allowed for this project. In addition, the quantification of the uncertainty in the TRISO buffer thickness was estimated to be small but this was done with a crude study and this might warrant a more thorough study as well. The buffer thickness uncertainty is not likely to be important but it would be good to confirm this.

FSV fuel compacts and a regular FSV fuel element were analyzed with MCNP5 for lattice-based "2-particle" and "4-particle" fuel for comparison to the modified version of HELIOS that was capable of analyzing TRISO fuel configurations. The HELIOS analyses were performed by SSP. At the time of this report, the differences between HELIOS and MCNP5 were on the order of 1% but this is expected to decrease as inconsistencies between the two analyses are identified and corrected.

Given all these uncertainties, full-core FSV configurations were developed for two initial critical configurations – a cold, clean critical loading and a critical configuration at 70% power. The MCNP5 calculations for the cold core were not very good for the eigenvalue (~1 % high with homogeneous fuel) but showed reasonable agreement for the axial flux distribution. However,

the eigenvalue for the 70% power configuration was reasonable, agreeing within .7% when heterogeneous fuel was modeled. The coupled MCNP5-RELAP simulation yielded reasonable agreement with predicted temperatures from a GA analysis.

Analyses were also done for the pulsed neutron experiments that were conducted by GA for the initial FSV core. MCNP5 was used to model these experiments and reasonable agreement with measured results has been observed. This work is continuing as part of the doctoral studies of Ben Betzler, a graduate student at the UM.

## IX. References

- [1] J. R. Brown, R. Hackney, V. Malakhof, and W. A. Simon, "Physics Testing at Fort St. Vrain – A Review," Nucl. Sci. Eng. 97, 104-122, 1987.
- [2] W. Pfeiffer, J. R. Brown, and A. C. Marshall, "Analysis and Results of Pulsed-Neutron Experiments Performed on the Fort St. Vrain High-Temperature Gas-Cooled Reactor," Nuclear Technology 27, 1975.
- [3] G. Yesilyurt, J. C. Lee, and W. R. Martin, "A Coupled Monte Carlo / Collision Probability Method for VHTR Analysis," Trans. Am. Nucl. Soc. 99, 753-754, Reno, NV, 2008.
- [4] Monte Carlo Team, "MCNP – A General Monte Carlo N-Particle Transport Code, Version 5," LA-UR-03-1987, Los Alamos National Laboratory (2003).
- [5] C. A. Wemple, H-N. M. Gheorghiu, R. J. J. Stamm'ler, and E. A. Villarino, "Recent Advances in the HELIOS-2 Lattice Physics Code," Proceedings of the International Conference on the Physics of Reactors (PHYSOR 2008), Interlaken, Switzerland (2008).
- [6] Sanchez, R., "Renormalized treatment of the double heterogeneity with the method of characteristics," PHYSOR2004, Chicago, 2004.
- [7] L. Pogosbekyan, G. Y. Kim, K. S. Kim, J. Y. Cho, and H. G. Joo, "Resolution of double heterogeneity in direct transport calculation employing subgroup method and method of characteristics," PHYSOR08, Interlaken, 2008.
- [8] L. L. Taylor, "Fort Saint Vrain HTGR (Th/U carbide) Fuel Characteristics for Disposal Criticality Analysis," DOE Report DOE/SNF/REP-060 (2001).
- [9] A. M. Baxter, email and telephone communications, October-November, 2010.
- [10] FSAR, "Fort St. Vrain Final Safety Analysis Report," General Atomic Report (1976).
- [11] General Atomics, "Public Service Company of Colorado 330-MW(E) High-Temperature Gas-Cooled Reactor Research and Development Program: Quarterly Progress Report for the Period Ending December 31, 1970," General Atomics Report GA-10444 (1971).
- [12] A. M. Baxter, D. McEachern, D. L. Hanson, and R. E. Vollman, "FSV Experience in Support of GT-MHR Reactor Physics, Fuel Performance, and Graphite," GA-A21925, November 1994.
- [13] R. J. Kapernick and R. J. Nirschl, "Fuel Fabrication Acceptance Report FSV – Initial Core," Gulf General Atomic report Gulf-GA-B12697 UC-80, December 1, 1973.

- [14] A. C. Marshall and J. R. Brown, "Loading of Fuel and Reflector Elements in the Fort St. Vrain Initial Core," Gulf General Atomic report GA-A13101 UC-77, November 1, 1974.
- [15] B. R. Betzler, W. R. Martin, and J. C. Lee, "MCNP5 Analysis of the Fort St. Vrain High-Temperature Gas-Cooled Reactor," Trans. Am. Nucl. Soc. 102, 515-516, San Diego, CA (June 2010).
- [16] G. Van Rossum, "Python 2.6.2," Python Software Foundation (2010).
- [17] The RELAP5-3D Code Development Team, "ATHENA Code Manual," INEEL-EXT-98-00834, Rev. 2.2, Idaho National Engineering and Environmental Laboratory (2003).
- [18] M. R. Wagner, "GAUGE: A Two-Dimensional Few Group Neutron Diffusion-Depletion Program for a Uniform Triangular Mesh," GA-8307, General Atomics (1968).
- [19] A. C. Marshall and J. R. Brown, "Neutron Flux Distribution Measurement in the Fort St. Vrain Initial Core (Results of the Fort St. Vrain Start-up Test A-7)," GA-A13176, General Atomic (1975).
- [20] H. Kraetsch and M. R. Wagner, "GATT: A Three Dimensional Few-Group Neutron Diffusion Theory Program for a Hexagonal-z Mesh," GA-8547, General Atomic (1969).
- [21] B. R. Betzler, E. E. Sunny, J. C. Lee and W. R. Martin, "Coupled Nuclear-Thermal-Hydraulic Calculations for Fort St. Vrain Reactor," Proc. 14th International Topical Meeting on Nuclear Reactor Thermal-hydraulics (NURETH-14), September 25-29, 2011, Toronto, Canada.
- [22] B. R. Betzler, J. C. Lee, and W. R. Martin, "MCNP5 Analysis of Fort St. Vrain High-Temperature Gas-Cooled Reactor", Trans Am. Nucl. Soc. 102, 515 (2010).
- [23] G. Yesilyurt, K. Banerjee, E. De Villele, J. C. Lee and W. R. Martin, "Coupled Nuclear-Thermal-Hydraulic Calculations for VHTRs," Trans Am. Nucl. Soc. 102, 519 (2010).
- [24] General Atomics Private Data.
- [25] M. Wagner, and J. Dorsey, "GATT-2X, An External Source Version of the Three Dimensional Diffusion Theory Program, GATT-2," General Atomics unpublished data.
- [26] R. J. Nirschl, "Three Dimensional Depletion Analysis for the 'As-Built' FSV Initial Core," General Atomics Report, GA-A13100, (1975).
- [27] S. R. Ross, J. R. Brown, and R. J. Nirschl, "Startup Physics Tests at Fort St. Vrain," GA-A13487, General Atomic (1975).
- [28] J. P. Dorsey and R. Froehlich, "GAMBLE-5: A Program for the Solution of," GA-8188, General Atomic (1967).
- [29] Y. Li and W. Ji, "A Collective Dynamics-based Method for Initial Pebble Packing in Pebble Flow Simulation", M&C 2011, Rio de Janeiro, Brazil (2011).
- [30] W.R. Martin and W. Ji, "Sampling TRISO Particles for Fort St. Vrain," Informal Report (2010).
- [31] A. T. Pavlou, B. R. Betzler, T. P. Burke, J. C. Lee, W. R. Martin, W. N. Pappo, and E. E. Sunny, "Eigenvalue Sensitivity Studies for the Fort St. Vrain High Temperature Gas-Cooled

Reactor to Account for Fabrication and Modeling Uncertainties," Proc. American Nuclear Society Reactor Physics Topical Meeting, PHYSOR-2012, Knoxville, TN, April 2012.

## **X. Students Supported by the Contract**

The following students were supported by the grant:

- Ms. Eva Sunny – graduate student.
- Mr. Ben Betzler – graduate student.
- Mr. Andrew Pavlou – graduate student.
- Mr. Wilson Pappo – undergraduate student, graduated April 2012.
- Mr. Timothy Burke – undergraduate student, graduated April 2012.

## **XI. Publications Directly Related to the Contract**

The following publications involve research supported by the grant:

1. B.R. Betzler, W.R. Martin, and J.C. Lee, "Modeling of the FSV HTGR with MCNP," poster presentation at the VHTR R&D Technical Review Meeting, Denver, CO (April 2010).
2. B.R. Betzler, W.R. Martin, and J.C. Lee, "MCNP5 Analysis of the Fort St. Vrain High-Temperature Gas-Cooled Reactor," Trans. Am. Nucl. Soc. 102, 515-516, San Diego, CA (June 2010).
3. B. R. Betzler, E. E. Sunny, J. C. Lee, W. R. Martin, "Coupled Nuclear-Thermal-Hydraulic Calculations for the Fort St. Vrain Reactor," poster presentation at the VHTR R&D Technical Review Meeting, Albuquerque, NM (April 2011).
4. B. R. Betzler, A. T. Pavlou, E. E. Sunny, T. P. Burke, W. N. Pappo, J. C. Lee, W. R. Martin, "Neutronic Sensitivity Studies in Support of the Fort St. Vrain Reactor Benchmark," poster presentation at the R&D VHTR Technical Review Meeting, Albuquerque, NM (April 2011).
5. Benjamin R. Betzler, Eva E. Sunny, John C. Lee and William R. Martin, "Coupled Nuclear-Thermal-Hydraulic Calculations for Fort St. Vrain Reactor," Proc. 14th International Topical Meeting on Nuclear Reactor Thermalhydraulics (NURETH-14), September 25-29, 2011, Toronto, Canada.
6. A. T. Pavlou, B. R. Betzler, T. P. Burke, J. C. Lee, W. R. Martin, W. N. Pappo, and E. E. Sunny, "Eigenvalue Sensitivity Studies for the Fort St. Vrain High Temperature Gas-Cooled Reactor to Account for Fabrication and Modeling Uncertainties," Proc. American Nuclear Society Reactor Physics Topical Meeting, PHYSOR-2012, Knoxville, TN, April 2012.
7. A. T. Pavlou, B. R. Betzler, T. P. Burke, J. C. Lee, W. R. Martin, W. N. Pappo, and E. E. Sunny, "Eigenvalue Sensitivity Studies for the Fort St. Vrain VHTR Benchmark," poster presentation at the VHTR R&D Technical Review Meeting, Salt Lake City, UT (May 2012).
8. B. R. Betzler, W. R. Martin, and J. C. Lee, "Simulation of Fort St. Vrain Pulsed Neutron Experiments with MCNP5," poster presentation at the VHTR R&D Technical Review Meeting, Salt Lake City, UT (May 2012).

## **XII. Other Publications**

The following publications involve research by students who were supported by the grant:

1. A.T. Pavlou, F.B. Brown, W.R. Martin, and B.C. Kiedrowski, "Comparison of Discrete and Continuous Thermal Neutron Scattering Treatments in MCNP5," Proc. American Nuclear Society Reactor Physics Topical Meeting, PHYSOR-2012, Knoxville, TN, April 2012.
2. C. Perfetti and W. Martin, B. Rearden, and M. Williams, Development of Continuous-Energy Eigenvalue Sensitivity Coefficient Calculation Methods in the SHIFT Monte Carlo Code," Proc. American Nuclear Society Reactor Physics Topical Meeting, PHYSOR-2012, Knoxville, TN, April 2012.
3. C. Perfetti and W. Martin, B. Rearden, and M. Williams, Determining Importance Weighting Functions for Contribution Theory Eigenvalue Sensitivity Coefficient Methodologies," Proc. American Nuclear Society Reactor Physics Topical Meeting, PHYSOR-2012, Knoxville, TN, April 2012.
4. E. E. Sunny, F. B. Brown, B. C. Kiedrowski, W. R. Martin, "Temperature Effects of Resonance Scattering for Epithermal Neutrons in MCNP," Proc. American Nuclear Society Reactor Physics Topical Meeting, PHYSOR-2012, Knoxville, TN, April 2012.